

1 **Response to reviewers**

2 *We are **grateful and thank** Reviewer #2 and Associate Editor for thorough assessment of our manuscript*  
3 *and for providing us constructive comments and suggestions.*

4 *In the revised version, **all the comments and suggestions have been taken into account** and changes*  
5 *have been made to improve the presentation.*

6 *We now add point-by-point reply (in italics, in red color fonts) to the comments and suggestions of the*  
7 *reviewer #2 and Associate Editor and make clear where and what changes have been made in the revised*  
8 *version of the manuscript.*

9

10 **Reviewer #2**

11 **Major suggestion**

12 **Comment 1:** The authors have adequately addressed all but one of my comments. In response to my  
13 comment on Figure 2, the authors state:

14 “The revised Figure 2d shows the portion of the gully system that was selected for measurement.”

15 But the revised Figure 2d is nearly identical to the original Figure 2d, and this doesn’t address the issue I  
16 raised in the original review: the fans shown here clearly interfinger and there appears to be a lot of  
17 evidence of crosscutting.

18 Perhaps you could annotate the figure with an outline of the gully system(s) you investigated? This would  
19 help to illustrate what you mean with the text on lines 152-154.

20 **Response 1:** *Done. As suggested, we have annotated the gully systems that were investigated in this study.*  
21 *Please see the revised figure 2. Also, in the caption of Figure 2, we have added the following:*

22 *‘The dashed lines show the gully systems that were investigated in this study.’*

23 *Please see line no. 126-127.*

24 **Minor suggestions**

25 **Comment 1:** Responding to the author’s responses on comments 9 and 12: The lighting and shadows  
26 make it impossible to tell from Fig 4 whether these gullies are V or U shaped, so the reader has to take

27 your word for it. For example, if it weren't for the label I might have assumed that the gullies in Figure  
28 4d were an example of a U-shape. A topographic cross-section would be helpful for illustrating the  
29 differences.

30 **Response 1:** *Done. As suggested, we have added a 'topographic profile' to illustrate the V-shaped*  
31 *incision. We have added the following in the caption of Figure 4 (line no. 218-219):*

32 *Note the topographic profile (A-A') in Figure 4e that illustrates V-shaped incision of the gully channel.*

33 **Comment 2:** Line 285: "deposits are having an elongated" -> "deposits have an elongated".

34 **Response 2:** *Done. Changed 'are having' to 'have'. Please see line no. 336.*

35 **Comment 3:** Line 366: I suggest changing "It is likely that the present-day sublimation of CO<sub>2</sub> ice on  
36 Mars provided" to "Present-day sublimation of CO<sub>2</sub> ice on Mars may have provided" (also in the abstract)

37 **Response 3:** *Done. Changed 'It is likely that the present-day sublimation of CO2 ice on Mars provided'*  
38 *to 'Present-day sublimation of CO2 ice on Mars may have provided' at both the places. Please see line*  
39 *nos. 418-419 and 25.*

40 **Comment 4:** Line 379: should "multiple formative mechanisms" be "multiple formative environments"?  
41 In the next paragraph you suggest that all of the gully systems were formed by debris flows (i.e., the same  
42 formative mechanism). I think that you are proposing that the difference is the geologic  
43 setting/environment, not the erosive process.

44 **Response 4:** *Agree. As suggested, we have changed 'multiple formative mechanisms' to 'multiple*  
45 *formative environments'. Please see line no. 432.*

46 **Comment 5:** Figures The figures (particularly the plots) are low resolution and appear somewhat  
47 pixelated. This may just be an issue in the PDF I am reviewing, but you may want to check prior to  
48 publication.

49 **Response 5:** *Sure. We have rechecked the resolution of the plots. They do not get pixelated at zoom level*  
50 *up to 150%.*

51 **Comment 6:** Figure 6: I still don't think this figure adds much. The interesting parts are already presented  
52 in Figure 5 (and the figure isn't really used other than lines 238-243). If you do keep the figure, I suggest  
53 the following: (1) add labels "Bedrock" and "LDM" to the Figure to make it more obvious without  
54 needing to read the caption. (2) Also move (a) and (b) to the upper left of each frame for consistency with  
55 other figures. (3) rotate the labels along the diagonal by ~30° to make it more obvious that they are  
56 referring to the columns.'

57 **Response 6:** Done. As suggested, we have (a) added labels 'Bedrock' and 'LDM/glacial deposits' to  
58 figures 'a' and 'b', respectively, (b) moved 'a' and 'b' to the upper left of each frame, and (3) rotated the  
59 labels diagonally by 30° to illustrate that the labels correspond to the columns. Please see the revised  
60 Figure 6.

61

62 **Associate Editor**

63 **Line comments:**

64 **Comment 1:** L14: either 'consisting of ice' or 'comprising ice'

65 **Response 1:** Done. Changed to 'consisting of ice'. Please see line no. 14.

66 **Comment 2:** L17: alcove and fan > the alcoves and fans

67 **Response 2:** Done. Changed 'alcove and fan' to 'the gully alcoves and fans'. Please see line no. 17.

68 **Comment 3:** L20: that mean gradient > that the mean gradient

69 **Response 3:** Done. Added 'the'. Please see line no. 20.

70 **Comment 4:** L33: incised into the > incised into:

71 **Response 4:** Done. Deleted 'the'. Please see line no. 33.

72 **Comment 5:** L34-35: The citations currently used are for one specific type of glacial deposit (GLFs),  
73 which don't seem to be the focus of this manuscript. More appropriate would be references to LDAs. But  
74 more specifically papers which show the glacier-gully interactions. For example Conway et al. 2018, de  
75 Haas et al. 2017 etc.

76 **Response 5:** Done. Changed 'Hubbard et al., 2011; Souness et al., 2012; Souness and Hubbard, 2012'  
77 to 'Conway et al., 2018' and 'de Haas et al., 2019a'. Please see line no. 34-35.

78 **Comment 6:** L47: (VFF) > (VFFs)

79 **Response 6:** Done. Changed 'VFF' to 'VFFs'. Please see line no. 46.

80 **Comment 7:** L48: extent of latitudes > latitude ranges (It would be good to state the latitude range here.)

81 **Response 7:** Done. Added 'between 30°-60°'. Please see line no. 47.

82 **Comment 8:** L49: This is the first in-text use of lobate debris apron, so define LDA acronym here.

83 **Response 8:** Done. Defined 'LDA as lobate debris aprons' at 48.

84 **Comment 9:** L49: fill > fills

85 **Response 9:** Done. Changed 'fill to 'fills''. Please see line no. 49.

86 **Comment 10:** L51: Conway et al. 2018 citation is not a suitable reference for this statement. You could  
87 refer to SHARAD papers, which infer high purity ice and thin debris cover. E.g.:

88 Holt et al. 2008 <https://doi.org/10.1126/science.1164246>; Plaut et al 2009  
89 <https://doi.org/10.1029/2008GL036379>; Petersen et al. 2018 <https://doi.org/10.1029/2018GL079759>

90 **Response 10:** Done. Replaced 'Conway et al., 2018' with 'Plaut et al., 2009'. Please see line no. 50.  
91 *The suggested reference has been added in the list of references.*

92 **Comment 11:** L70 & 81: morphology and morphometry > morphologies and morphometries

93 **Response 11:** Done. Changed 'morphology and morphometry' to 'morphologies and morphometries'.  
94 *Please see line no. 69 and 80.*

95 **Comment 12:** L75: Gullies by studying long profiles of gullies > gullies by studying their long profiles

96 **Response 12:** Done. Changed 'gullies by studying long profiles of gullies' to 'gullies by studying their  
97 long profiles'. Please see line no. 74.

98 **Comment 13:** L81: southern hemisphere > southern hemisphere of Mars

99 **Response 13:** Done. Added 'of Mars' after 'southern hemisphere'. Please see line no. 80.

100 **Comment 14:** L83: digital terrain model (DTM) > digital terrain models (DTMs)

101 **Response 14:** Done. Changed 'digital terrain model (DTM)' to 'digital terrain models (DTMs)'. Please  
102 see line no. 82.

103 **Comment 15:** L88: DTMs are produced > we produced DTMs with

104 **Response 15:** Done. Changed 'DTMs are produced' to 'we produced DTMs'. Please see line no. 87.

105 **Comment 16:** Table 1, row 'Artik': See L49 comment about defining LDA earlier, and remove LDA  
106 definition from here.

107 **Response 16:** Done. Removed 'LDA' definition from Table 1.

108 **Comment 17:** L107-114: There are currently no in-text references to Fig 2b-d, please add

109 **Response 17:** Done. Added in-text references for Fig. 2b, 2c and 2d. Please see line no. 106, 113, and  
110 116.

111 **Comment 18:** L107: 'alcoves on the walls': would it be better to say 'topographic depressions'? Alcoves  
112 is confusing if you don't necessarily mean gully alcoves.

113 **Response 18:** Done. Changed 'alcoves' to 'gully alcoves'. Please see line no. 106. Also, checked the  
114 entire manuscript for consistency. 'Alcoves' have been changed to 'Gully alcoves'.

115 **Comment 19:** L109-111: see above comments - you could just change alcoves to 'topographic  
116 depressions' to avoid this confusion?

117 **Response 18:** We have changed 'alcoves' to 'gully alcoves' in the entire manuscript.

118 **Comment 19:** L114: Could do with an extra phrase here - that they are also inferred to incise LDM? Your  
119 explanation in the response to reviewers was helpful in this regard, and this explanation would benefit  
120 from that addition in the manuscript itself.

121 **Response 19:** Done. As suggested, we have added 'and are also inferred to incise LDM deposits'. Please  
122 see line no. 113-114.

123 **Comment 20:** L115: Add reference to Fig 2d

124 **Response 20:** Done. Added in-text reference to Fig. 2d. Please see line no. 116.

125 **Comment 21:** L115: listed in LDM/glacial deposits > listed in criterion 1 (LDM/glacial deposits)

126 **Response 21:** Done. Added 'criterion 1' before LDM/glacial deposits. Please see line no. 115.

127 **Comment 22:** L122: delete the in 'the Terra Sirenum'

128 **Response 22:** Done. Deleted 'in the Terra Sirenum'. Please see line no. 122.

129 **Comment 23:** L122: delete 'evidence of'. The polygons are visible and are themselves evidence of LDM.

130 **Response 23:** Done. Deleted 'Evidence of'. Please see line no. 122.

131 **Comment 24:** L133: 'dimensionless variables' – give a couple of examples here?

132 **Response 24:** Done. Added form factor, elongation ratio, and circularity ratio as examples of  
133 dimensionless variables. Please see line no. 134.

134 **Comment 25:** Table 2 (and Figs 5, 6 & Table 3): Perimeter > Alcove Perimeter

135 **Response 25:** Done. Changed 'Perimeter' to 'Alcove Perimeter' in Figs 5 and 6, and in Table 2 and 3.

136 **Comment 26:** L155: HiRISE DTM that was used > HiRISE DTMs used for  
137 *Response 26: Done. Changed 'HiRISE DTM that was used' to 'HiRISE DTMs used for'. Please see line*  
138 *no. 155-156.*

139 **Comment 27:** L157&158: source area is > source areas are  
140 *Response 27: Done. Changed 'source area is' to 'source areas are' at both the places. Please see line*  
141 *no. 158 and 159.*

142 **Comment 28:** L167: Conway et al. 2015 isn't a seminal reference for CDA – provide one for CDA and/or  
143 make clear that this citation refers specifically to gullies.  
144 *Response 28: Done. We have moved Conway et al., 2015 as the reference for line no. 171. Further,*  
145 *McLachlan, 2004 has been added as a reference for CDA. Please see line no. 168.*

146 *McLachlan, G. J.: Discriminant analysis and statistical pattern recognition, John Wiley & Sons, 2005.*

147 **Comment 29:** L174:  
148 (a) LDM and VFFs > LDM and/or VFFs (you go on to say some aren't affected by both)  
149 (b) Consider whether 'glacial deposits' would be better than VFFs. Are there locations where there are  
150 arcuate ridges and no accompanying VFFs? If so, 'glacial deposits' would be more appropriate as it covers  
151 both arcuate ridges and VFFs.  
152 *Response 29: (a) Done. Added 'and' after LDM. Please see line no. 175.*  
153 *(b) VFFs were observed in nearly all the studied craters. So, we keep both arcuate ridges and VFFs.*

154 **Comment 30:** L177: 4 craters out of 24 craters > 4 craters out of 24 craters influenced by LDM and/or  
155 VFFs (see also comment 174b above)  
156 *Response 30: We cannot use and/or here because for these craters VFFs were not observed. These craters*  
157 *have gullies only influenced by LDM. Hence, we have not changed anything here in the manuscript.*

158 **Comment 31:** L233-234: Please fully describe the boxplot elements. e.g. Box shows interquartile range,  
159 central horizontal bar shows median, and whiskers show range.  
160 *Response 31: Done. As suggested, we have rephrased the Figure caption as:*  
161 *The boxplot presented here shows interquartile range, central horizontal bar shows median, and whiskers*  
162 *show range of values of alcove/fan geometry, relief, gradient, and dimensionless variables of gullies*  
163 *incised into LDM/glacial deposits (pink) and bedrock (green).*

164 *Please see line no. 261-263.*

165 **Comment 32:** L242: Define threshold for ‘very strong positive correlation’

166 **Response 32:** *Done. Added ‘(>0.9)’ as threshold for very strong positive correlation. Please see line no.*  
167 *271.*

168 **Comment 33:** L245: What correlation coefficient is this? Pearsons?

169 **Response 33:** *Yes, Pearson correlation. We have added ‘Pearson’ in caption of Fig. 6 and in the text.*  
170 *Please see line no. 295.*

171 **Comment 34:** L246: Values approaching -1 are also strong, so reword this. e.g. 'Values approaching  
172 either 1 or -1 have stronger correlations. Zero indicates no correlation.'

173 **Response 34:** *Done. As suggested, we have added ‘Values approaching either 1 or -1 have stronger*  
174 *correlations. Zero indicates no correlation’ in the caption of Fig. 6. Please see line no. 296.*

175 **Comment 35:** L255: Is this an explanation of the 'weight'? If so, explain this after the first mention of  
176 weights (i.e. line 253). e.g. on line 253, you could say weight values indicate the discriminator power in  
177 separating between...! Then here, '...relief ratio (fan) have nearly 1/5 or greater (but less than 1/3) of the  
178 weight of alcove perimeter...'

179 **Response 35:** *Done. As suggested, we have added the following: ‘ Here, the weight values indicate the*  
180 *discriminator power in separating between the gullies formed in LDM/glacial deposits and bedrock’.*  
181 *Please see line no. 303-304.*

182 *In the next line, rephrased the sentence as follows: ‘The remaining variables such as fan relief, fan length,*  
183 *relief ratio (alcove), alcove width, and relief ratio (fan) have nearly 1/5 or greater (but less than 1/3) of*  
184 *the weight of alcove perimeter discriminatory power in separating between the gullies formed in*  
185 *LDM/glacial deposits and bedrock’.* Please see line no. 304-307.

186 **Comment 36:** L261: Discussions > Discussion

187 **Response 36:** *Done. Changed ‘Discussions’ to ‘Discussion’.* Please see line no. 312.

188 **Comment 37:** L270: alcoves > gully alcoves

189 **Response 37:** *Done. Changed ‘alcoves’ to ‘gully alcoves’.* Please see line no. 321.

190 **Comment 38:** L272: Care needed with these citations: most early papers didn't infer high ice purity  
191 (instead preferring a rock glacier model). High confidence of ice content only came later, particularly  
192 with the radar studies.

193 **Response 38:** *As suggested, we have changed 'Mangold, 2003; Levy et al., 2009a; Morgan et al., 2009'*  
194 *to 'Baker et al., 2010; Plaut et al., 2009'. Please see line no. 325.*

195 *Baker, D. M. H, James W. H., and David R. M.: Flow patterns of lobate debris aprons and lineated valley*  
196 *fill north of Ismeniae Fossae, Mars: Evidence for extensive mid-latitude glaciation in the Late Amazonian,*  
197 *Icarus 207, 186-209, 2010, doi: <https://doi.org/10.1016/j.icarus.2009.11.017>.*

198 **Comment 39:** L273: interpreted to be comprised of > interpreted to comprise

199 **Response 39:** *Done. Changed 'interpreted to be comprised' to interpreted to comprise'. Please see line*  
200 *no. 324.*

201 **Comment 40:** L285: are having an elongated, V-shaped cross-section in their mid-section > do have  
202 elongated, V-shaped cross-sections in their mid-sections

203 **Response 40:** *Done. Changed 'are having an elongated, V-shaped cross-section in their mid-section' to*  
204 *'do have an elongated, V-shaped cross section in their mid-sections'. Please see line no. 336.*

205 **Comment 41:** L287: perimeters and reliefs Please check pluralisation throughout

206 **Response 41:** *Done. Changed 'perimeter and relief' to 'perimeters and reliefs'. Please see line no. 338.*

207 *Additionally, we have checked the entire manuscript for pluralization and corrected, wherever required.*

208 **Comment 42:** L288: citations for 'previous studies'?

209 **Response 42:** *Done. Added 'Aston et al., 2011' as the reference for previous studies. Please see line no.*  
210 *340.*

211 **Comment 43:** L370: latitudes > latitudes on Mars

212 **Response 43:** *Done. Added 'on Mars' after latitudes. Please see line no. 423.*

213 **Comment 44:** L394: ESurfD > ESurf

214 **Response 44:** *Done. Changed 'ESurfD' to 'ESurf'. Please see line no. 448.*

215

216

217



218 **Morphologic and Morphometric Differences between Gullies Formed**  
219 **in Different Substrates on Mars: New Insights into the Gully**  
220 **Formation Processes**

221 Rishitosh K. Sinha<sup>1,2</sup>, Dwijesh Ray<sup>1</sup>, Tjalling De Haas<sup>3</sup>, Susan J. Conway<sup>4</sup>, Axel Noblet<sup>4</sup>

222 <sup>1</sup> Physical Research Laboratory, Ahmedabad 380009, Gujarat, India

223 <sup>2</sup> Indian Institute of Technology, Gandhinagar 382355, Gujarat, India

224 <sup>3</sup> Faculty of Geoscience, Universiteit Utrecht, Princetonlaan 8a, 3584 CB Utrecht, the Netherlands

225 <sup>4</sup> Nantes Université, Université d'Angers, Le Mans Université, CNRS UMR 6112 Laboratoire de Planétologie et Géosciences,

226 France

227

228 *Correspondence to:* Rishitosh K. Sinha (rishitosh@prl.res.in)

229 **Abstract.** Martian gullies are kilometer-scale geologically young features with a source alcove, transportation channel, and  
230 depositional fan. On the walls of impact craters, these gullies typically incise into bedrock or surfaces modified by latitude  
231 dependent mantle (LDM; inferred as consisting of ice and admixed dust) and glaciation. To better understand the differences  
232 in alcoves and fans of gullies formed in different substrates and infer the flow types that led to their formation, we have  
233 analyzed the morphology and morphometry of 167 gully systems in 29 craters distributed between 30°S and 75°S. Specifically  
234 we measured length, width, gradient, area, relief, and relief ratio of the gully alcoves and fans, Melton ratio, relative concavity  
235 index, and perimeter, form factor, elongation ratio and circularity ratio of the gully alcoves. Our study reveals that gully alcoves  
236 formed in LDM/glacial deposits are more elongated than the gully alcoves formed in bedrock, and possess a distinctive V-  
237 shaped cross section. We have found that the mean gradient of fans formed by gullies sourced in bedrock is steeper than the  
238 mean gradient of fans of gullies sourced in LDM/glacial deposits. These differences between gullies were found to be  
239 statistically significant and discriminant analysis has confirmed that alcove perimeter, alcove relief and fan gradient are the  
240 most important variables for differentiating gullies according to their source substrates. The comparison between the Melton  
241 ratio, alcove length and fan gradient of Martian and terrestrial gullies reveals that Martian gully systems were likely formed  
242 by terrestrial debris-flow like processes. ~~Present-day sublimation of CO<sub>2</sub> ice on Mars may have provided~~ the adequate flow  
243 fluidization for the formation of deposits akin to terrestrial debris-flow like deposits.

**Formatted:** Subscript

**Deleted:** It is likely that the present-day sublimation of CO<sub>2</sub> ice on Mars provided

244 **1 Introduction**

245 Gullies are found on steep slopes polewards of about 30° latitude in both hemispheres on Mars and manifest as kilometer-  
246 scale, geologically young features (formed within the last few million years) comprising an alcove, channel, and depositional  
247 fan (Malin and Edgett, 2000; Dickson et al., 2007; Reiss et al., 2004; Schon et al., 2009). Gullies occur in a wide assortment  
248 of settings, varying from the walls and central peaks of craters to walls of valleys, and steep faces of dunes, hills and polar pits

251 (e.g. Balme et al., 2006; Dickson et al., 2007; Dickson and Head, 2009; Conway et al., 2011, 2015; Harrison et al., 2015). On  
252 the walls of craters, gullies are found to have incised into (1) surfaces covered by latitude dependent mantle (LDM; e.g. Mustard  
253 et al., 2001; Dickson et al., 2012, 2015), (2) surfaces modified by former episodes of glaciation (Conway et al., 2018; de Haas  
254 2019a; Sinha and Vijayan, 2017), and (3) bedrock (e.g. Johnsson et al., 2014; de Haas et al., 2019a; Sinha et al., 2020). Detailed  
255 investigation of the gullies formed over these different substrates is key to understanding the intricacies of past processes by  
256 which these gullies have formed on Mars (Conway et al., 2015; de Haas et al., 2019a).

257 A variety of models have been proposed to explain the formation of gullies, which include: (1) dry flows triggered by  
258 sublimation of CO<sub>2</sub> frost (e.g. Cedillo-Flores et al., 2011; Dundas et al., 2012, 2015; Pilorget and Forget, 2016; de Haas et al.,  
259 2019b), (2) debris-flows of an aqueous nature (e.g. Costard et al., 2002; Levy et al., 2010; Conway et al., 2011; Johnsson et  
260 al., 2014; de Haas et al., 2019a; Sinha et al., 2020), and (3) fluvial flows (e.g. Heldmann and Mellon, 2004; Heldmann et al.,  
261 2005; Dickson et al., 2007; Reiss et al., 2011). To better understand the gully formation processes, morphometric investigation  
262 of gullies formed over different substrates needs to be undertaken at a level of detail previously not attempted.

263 The global distribution of gullies shows a spatial correlation with the landforms indicative of glaciation and LDM deposition  
264 on Mars (e.g. Levy et al., 2011; Dickson et al., 2015; Harrison et al., 2015; Conway et al., 2018; de Haas et al., 2019a; Sinha  
265 et al., 2020). With respect to glacial landforms, many gullies have formed into viscous flow features (VFFs) and they are found  
266 in the same latitude ranges between 30°-60° (e.g. Arfstrom and Hartmann, 2005; de Haas et al., 2019a). VFFs are defined as  
267 an umbrella term for glacial-type formations covering a broad range of landforms that include lobate debris aprons (LDAs),  
268 concentric crater fills (CCFs), and lineated valley fills (LVFs) (e.g. Squyres, 1978; Levy et al., 2009a; Baker et al., 2010;  
269 Hargitai, 2014). Together, they are inferred to be similar to terrestrial debris-covered glaciers (Plaut et al., 2009). With respect  
270 to LDM, gullies are mostly found on the pole-facing slopes of crater walls at lower mid-latitudes (30-45°) (e.g. Balme et al.  
271 2006; Kneissl et al. 2010; Harrison et al. 2015; Conway et al. 2017), wherein, LDM is found to be dissected (e.g. Mustard et  
272 al., 2001; Milliken et al., 2003; Head et al., 2003). In the higher latitudes (>45°), LDM is found to be continuous (e.g.  
273 Kreslavsky and Head, 2000), and gullies are evident at both the pole and equator facing slopes (e.g. Balme et al. 2006; Kneissl  
274 et al. 2010; Harrison et al. 2015; Conway et al. 2017). Gullies formed on the formerly glaciated walls of craters are fed from  
275 alcoves that do not extend up to the crater rim, and appear elongated to V-shaped, implying gully-channel incision into ice-  
276 rich, un lithified sediments (e.g. Aston et al., 2011; de Haas et al., 2019a). The alcoves, channels and fan deposits of gullies  
277 formed within craters covered by a smooth drape of LDM, are usually found to have experienced multiple episodes of LDM  
278 covering and subsequent reactivation of some of the pre-existing channels or formation of fresh channels within the draped  
279 LDM deposits (e.g. Dickson et al., 2015; de Haas et al., 2019a). Additionally, there are gullies that directly emanate from well-  
280 defined bedrock alcoves that cut into the crater rim in the absence of LDM and/or glacial deposits (e.g. Johnsson et al., 2014;  
281 de Haas et al., 2019a; Sinha et al., 2020). Gullies formed in these craters have alcoves with sharply defined crests and spurs,  
282 exposing the underlying bedrock, and meter-sized boulders are found throughout the gully system (e.g. Johnsson et al., 2014;

Deleted: the

Deleted: Hubbard et al., 2011; Souness et al., 2012; Souness and Hubbard, 2012

Deleted: extent of latitudes

Deleted: 8

Deleted: Conway et al., 2018

289 de Haas et al., 2019a; Sinha et al., 2020). Further, De Haas et al., 2015a found that the stratigraphy of the fans whose source  
290 area was in bedrock were more boulder-rich than those fans fed by catchments in LDM. The findings in these studies suggest  
291 that a more detailed investigation of the morphology and morphometry of the gullies formed over contrasting substrates is  
292 important for improving our understanding of the formative mechanisms of gullies.

293 In this work, we focus on addressing the following research questions:

294 (1) Do the morphologies and morphometries of gully systems formed in different substrates differ (i.e. LDM/glacial deposits  
295 and bedrock)?

Deleted: y

Deleted: y

296 (2) How do the morphometric characteristics of gullies formed on Mars compare to those formed by a range of processes on  
297 Earth, and what does that tell us about the formative processes of Martian gullies?

298 To parameterize the morphometry we will primarily study long profiles. Previously, only a few studies have analyzed the  
299 morphometric characteristics of the gullies by studying their long profiles (e.g. Yue et al., 2014; Conway et al., 2015; De Haas  
300 et al., 2015a; Hobbs et al., 2015). These studies have focused observations on a part of the gully system and suggested that the  
301 differences in the properties of substrate into which the gullies incise play a significant role in promoting the flows that led to  
302 gully formation. Hence, for a more detailed differentiation of the gully types and interpretation of the dominant flow type that  
303 led to gully formation on Mars, quantification of the morphometric characteristics of the entire gully system is crucial.

Deleted: of gullies

## 304 2 Study sites and datasets

305 We characterize the morphologies and morphometries of gullies in 29 craters distributed over the southern hemisphere of Mars  
306 between 30° S and 75° S latitude (Fig. 1). These 29 craters are selected based on the availability of publicly released High  
307 Resolution Imaging Science Experiment (HiRISE) stereo-pair based digital terrain models (DTMs) or the presence of suitable  
308 HiRISE stereo-pair images to produce a DTM ourselves. The HiRISE stereo-pair images are usually ~0.25 - 0.5 m/pixel  
309 (McEwen et al., 2007), so the DTM post spacing is ~1-2 m with vertical precision in the range of tens of centimeters (Kirk et  
310 al., 2008). Among the 29 gullied craters, publicly released DTMs are available for 25 craters  
311 (<https://www.uahirise.org/hiwish/maps/dtms.jsp> - last accessed 18th September 2021) (Table 1). For the remaining 4 craters,  
312 we produced DTMs with the software packages USGS ISIS and BAE Systems SocetSet (Table 1) (Kirk et al., 2008). We  
313 investigated HiRISE images of these 29 gullied craters for detailed morphological characterization of the substrate into which  
314 the crater wall gullies incise (Table 1).

Deleted: y

Deleted: y

Deleted: DTMs are produced

315

316

323 **Table 1.** Summary of the craters included in this study, their locations, number of gullies investigated from the crater, substrate  
 324 on the crater wall in which gullies have incised, key morphological attributes of the substrate, and IDs of HiRISE imagery and  
 325 DTM used for morphological and morphometric investigation of gullies in these craters.

Crater	Latitude	Longitude	No. of gullies	Substrate	Key morphological attributes	HiRISE ID	HiRISE DTM ID
Artik	34.8° S	131.02° E	2	LDM/glacial deposits	Polygons, V-shaped incisions, arcuate ridges, small-scale LDAs on the floor	ESP_020740_1450	DTEEC_012459_1450_012314_1450_A01
Asimov	47.53° S	4.41° E	4	LDM/glacial deposits	Polygons, V-shaped incisions, mantled alcoves/channels/fans, arcuate ridges, small-scale LDAs inside valleys	ESP_012912_1320	DTEEC_012912_1320_012767_1320_A01
Bunnik	38.07° S	142.07° W	8	LDM/glacial deposits	Polygons, V-shaped incisions, mantled alcoves/channels/fans, arcuate ridges	ESP_047044_1420	DTEEC_002659_1420_002514_1420_U01
Corozal	38.78° S	159.48° E	6	LDM/glacial deposits	Polygons, mantled alcoves/channels/fans, arcuate ridges, small-scale LDAs on the floor	PSP_006261_1410	DTEEC_006261_1410_014093_1410_A01
Dechu	42.23° S	158° W	8	LDM/glacial deposits	Polygons, mantled alcoves/channels/fans, arcuate ridges, small-scale LDAs on the floor	PSP_006866_1375	DTEED_023546_1375_023612_1375_A01
Dunkassa	37.46° S	137.06° W	5	LDM/glacial deposits	Polygons, V-shaped incisions, mantled alcoves/channels/fans, arcuate ridges, small-scale LDAs on the floor	ESP_032011_1425	DTEEC_039488_1420_039343_1420_A01
Hale	35.7° S	36.4° W	8	LDM/glacial deposits	Polygons, V-shaped incisions, mantled alcoves/channels/fans, talus slope deposits	PSP_003209_1445	DTEEC_002932_1445_003209_1445_A01
Langtang	38.13° S	135.95° W	5	LDM/glacial deposits	Polygons, V-shaped incisions, mantled alcoves/channels/fans, arcuate ridges, small-scale LDAs on the floor	ESP_030099_1415	DTEEC_024099_1415_023809_1415_U01

Deleted: lobate debris aprons ( Deleted: )

Moni	46.97° S	18.79° E	5	LDM/glacial deposits	Partly infilled alcoves, mantled fan surfaces, arcuate ridges	ESP_056862_1325	DTEEC_007110_1325_006820_1325_A01
Nybyen	37.03° S	16.66° W	8	LDM/glacial deposits	Polygons, mantled alcoves/channels/fans, arcuate ridges	ESP_059448_1425	DTEEC_006663_1425_011436_1425_A01
Palikir	41.56° S	157.87° W	5	LDM/glacial deposits	Polygons, V-shaped incisions, mantled alcoves/channels/fans, arcuate ridges, small-scale LDAs on the floor	ESP_057462_1380	DTEEC_005943_1380_011428_1380_A01
Penticton	38.38° S	96.8° E	7	LDM/glacial deposits	Polygons, V-shaped incisions, mantled alcoves/channels/fans, arcuate ridges, small-scale LDAs on the floor	ESP_029062_1415	DTEEC_001714_1415_001846_1415_U01
Selevac	37.37° S	131.07° W	8	LDM/glacial deposits	Polygons, mantled alcoves/channels/fans, small-scale flows on the floor	ESP_045158_1425	DTEEC_003252_1425_003674_1425_A01
Raga	48.1° S	117.57° W	4	LDM	Polygons, mantled alcoves/channels/fans	ESP_041017_1315	DTEEC_014011_1315_014288_1315_A01
Roseau	41.7° S	150.6° E	1	LDM	Polygons, mantled alcoves/channels/fans	ESP_024115_1380 / ESP_011509_1380	ESP_024115_1380_ESP_011509_1380*
Taltal	39.5° S	125.8° W	7	LDM/glacial deposits	Polygons, V-shaped incisions, mantled alcoves/channels/fans, arcuate ridges, small-scale LDAs on the floor	ESP_037074_1400 / ESP_031259_1400	ESP_037074_1400_ESP_031259_1400*
Talu	40.34° S	20.11° E	7	LDM/glacial deposits	Polygons, V-shaped incisions, mantled alcoves/channels/fans, arcuate ridges, small-scale LDAs on the floor	ESP_011817_1395	DTEEC_011817_1395_011672_1395_O01
Triolet	37.08° S	168.02° W	4	LDM/glacial deposits	Polygons, V-shaped incisions, mantled alcoves/channels/fans, arcuate ridges, small-scale LDAs on the floor	ESP_047190_1425	DTEEC_023586_1425_024008_1425_A01
Unnamed crater	32.31° S	118.55° E	4	LDM/glacial deposits	Polygons, mantled alcoves/channels/fans	PSP_006869_1475	DTEEC_021914_1475_022336_1475_U01

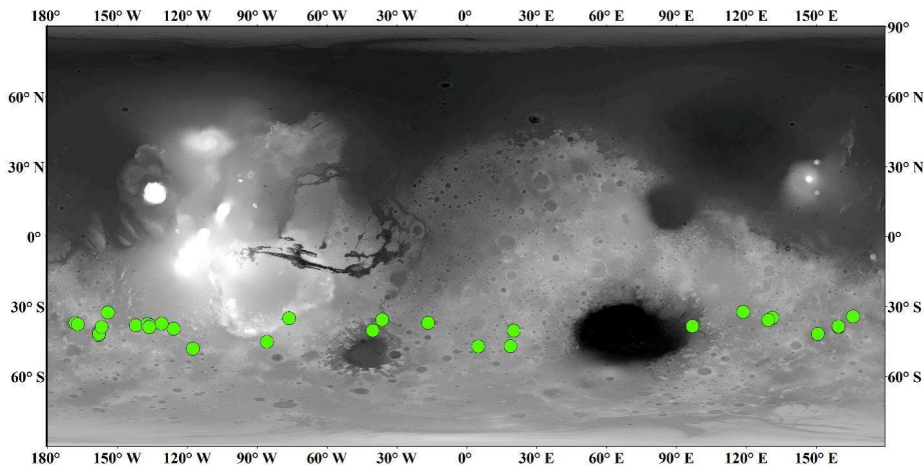
					s, arcuate ridges, small-scale LDAs on the floor		
Unnamed crater in the Argyre basin	40.3° S	40.4° W	6	LDM/glacial deposits	Polygons, mantled alcoves/channels/fans, arcuate ridges, small-scale LDAs on the floor	ESP_032047_1395	DTEEC_012795_1395_013507_1395_A01
Unnamed crater in the Newton basin	38.8° S	156.8° W	5	LDM	Polygons, V-shaped incisions, mantled alcoves/channels/fans	PSP_002686_1410	DTEEC_002620_1410_002686_1410_A01
Unnamed crater north of Corozal crater	38.53° S	159.44° E	5	LDM/glacial deposits	Polygons, mantled alcoves/channels/fans, small-scale LDAs on the floor	ESP_020884_1410	DTEEC_020884_1410_020950_1410_A01
Unnamed crater-1 in the Terra Sirenum	32.55° S	154.11° W	2	LDM	Mantled alcoves/channels/fans	PSP_007380_1470	DTEEC_010597_1470_007380_1470_U01
Unnamed crater-2 in the Terra Sirenum	38.88° S	136.36° W	6	LDM/glacial deposits	Polygons, V-shaped incisions, mantled alcoves/channels/fans, arcuate ridges, small-scale LDAs on the floor	ESP_020407_1410	DTEEC_022108_1410_022385_1410_A01
Istok	45.1° S	85.82° W	8	Bedrock	Alcove cut directly into the original crater-wall material, clasts embedded into fresh deposits on fan	ESP_056668_1345	DTEEC_040607_1345_040251_1345_A01
Galap	37.66° S	167.07° W	8	Bedrock	Alcove cut directly into the original crater-wall material, clasts embedded into fresh deposits on fan	ESP_059770_1420	DTEEC_048983_1420_048693_1420_U01
Gasa	35.73° S	129.4° E	7	Bedrock	Alcove cut directly into the original crater-wall material, clasts embedded into fresh deposits on fan	ESP_057491_1440	DTEEC_021584_1440_022217_1440_A01
Los	35.08° S	76.23° W	7	Bedrock	Alcove cut directly into the original crater-wall material,	ESP_020774_1445 / ESP_050127_1445	ESP_020774_1445_ESP_050127_1445*

					clasts embedded into fresh deposits on fan		
Unnamed crater-3 in the Terra Sirenum	34.27° S	165.71° E	7	Bedrock	Alcove cut directly into the original crater-wall material, clasts embedded into fresh deposits on fan	ESP_049261_1455 / ESP_049828_1455	ESP_049261_1455_ ESP_049828_1455*

328

329 (\*) DTMs are produced with the software packages USGS ISIS and BAE Systems SocetSet.

330



331 Figure 1: Locations of craters analyzed in this study (green circles). Background: Mars Orbiter Laser Altimeter gridded data, where  
 332 white is high elevation and black is low elevation, credit MOLA Science Team/NASA/JPL.

333

334 **3 Approach**

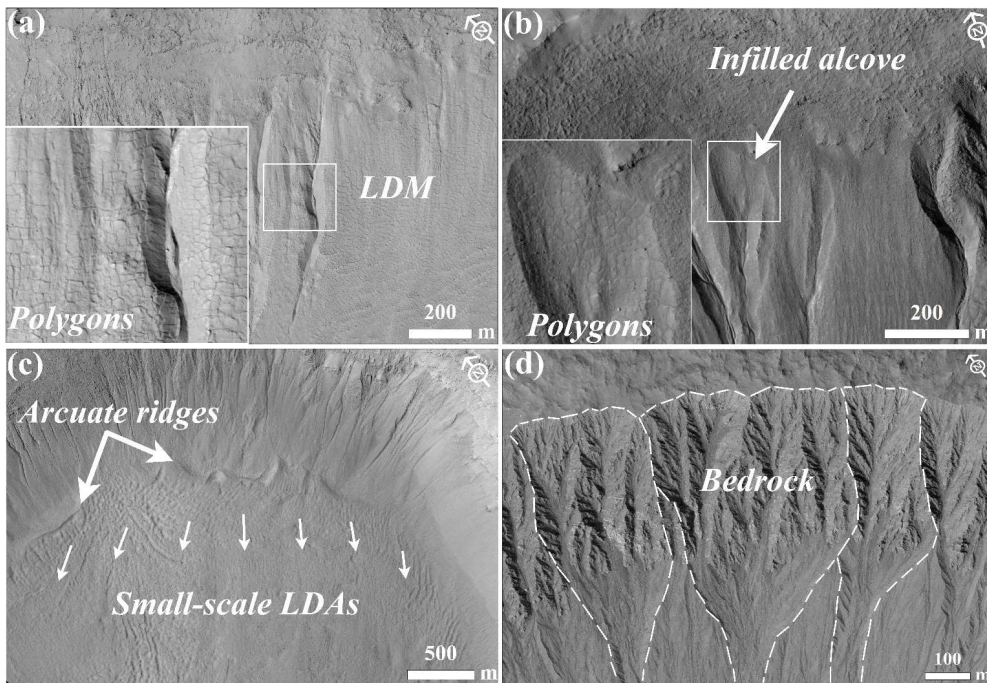
335 **3.1 Identification of substrate**

336 The substrate into which the gullies have incised is identified based on the following criteria:

- 337 1. LDM/glacial deposits: Any crater whose gullies incise walls that appear to be softened by the drape of smooth mantling  
 338 material with polygonal cracks is inferred to have LDM as the substrate within which gullies have incised (e.g. Mustard et al.,

339 2001; Kreslavsky and Head, 2002; Levy et al., 2009a; Conway et al., 2018; de Haas et al., 2019a) (Fig. 2a-b). The **gully** alcoves  
 340 on the walls of these craters may be partially to completely filled by LDM, and in some cases, polygonized LDM materials  
 341 may be seen covering the alcove walls (e.g. Christensen, 2003; Conway et al., 2018; de Haas et al., 2019a). These infilled  
 342 alcoves on the crater walls are not the alcoves of gullies formed within the LDM substrate; instead, they represent the alcoves  
 343 that were formed prior to the LDM emplacement epoch. Additionally, gullied craters that show evidence in the form of arcuate  
 344 ridges at the foot of the walls and VFFs that cover part or the entire crater floor are inferred to have been modified by one or  
 345 multiple episodes of glaciation (e.g. Arfstrom and Hartmann, 2005; Head et al., 2010; Milliken et al., 2003; Hubbard et al.,  
 346 2011) (Fig. 2c). These craters host gullies that are often partially or fully covered by LDM deposits **and are also inferred to**  
 347 **incise LDM deposits.**

348 2. Bedrock: Craters where the features listed in **criteria 1** (LDM/glacial deposits) are absent and where rocky material is  
 349 visible extending downwards from the crater rim (Fig. 2d). This rocky material usually outcrops as spurs and can be layered  
 350 or massive. The slopes can be smooth or covered with boulders, with concentrations of boulders at the slope toe.



351



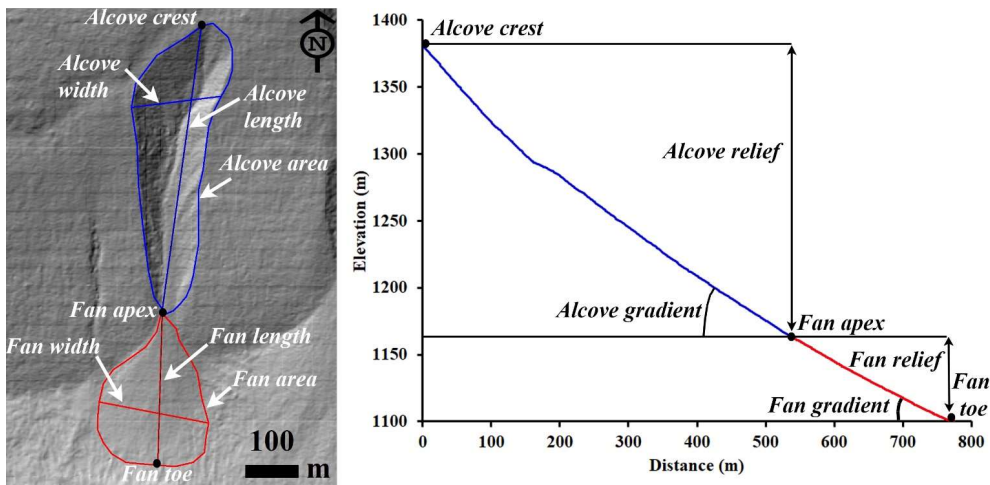
352 Figure 2: Examples of morphological evidence used to identify LDM, glacial deposits, and bedrock. (a) Smooth mantling material  
 353 inferred as LDM draped on the wall of Talu crater on the basis of polygonal cracks formed in the material. The bigger box is an  
 354 expanded view of the polygons seen over the region outlined by the smaller box. (HiRISE image ESP\_011817\_1395). (b) An infilled  
 355 alcove on the wall of an unnamed crater-2 in Terra Sirenum. Polygons in the infilled material suggests presence of LDM deposits  
 356 draped on the wall. The region shown in smaller box is expanded in the bigger box to show evidence of the polygons. (HiRISE image  
 357 ESP\_020407\_1410). (c) Glaciation inferred in the Corozal crater on the basis of arcuate ridges formed at the foot of the crater wall  
 358 and small-scale LDAs on the crater floor. Arrows indicate the downslope flow of LDAs on the floor. (HiRISE image  
 359 PSP\_006261\_1410). (d) Exposed fractured bedrock identified on the walls of Istok crater within which gully alcoves have incised.  
 360 The dashed lines show the gully systems within Istok crater that were investigated in this study. (HiRISE image ESP\_056668\_1345).  
 361 HiRISE image credit: NASA/JPL /University of Arizona.

Deleted: the  
 Deleted: Evidence of p

362

### 363 3.2 Morphometric variables

364 The measurements we made of each gully system include alcove area, alcove perimeter, alcove length, alcove width, alcove  
 365 gradient, fan area, fan length, fan width, and fan gradient (Fig. 3). In total, we derived 18 morphometric variables to  
 366 characterize each gully fan and its alcove. The morphometric variables are classified into geometry, relief, gradient, and  
 367 dimensionless variables (e.g. form factor, elongation ratio, and circularity ratio) and they are calculated with established  
 368 mathematical equations shown in Table 2. For the gradient measurement using the DTM, the topographic profile from (1) crest  
 369 of the alcove to the apex of the fan was extracted for the alcove, and (2) apex to foot of the fan was extracted for the fan.



370

371 Figure 3: Examples of morphometric variables estimated in this work. Left panel: HiRISE DTM (Id:  
 372 DTEEC\_002659\_1420\_002514\_1420) based hillshade. HiRISE DTM credit: NASA/JPL /University of Arizona. Right panel:

375 **Topographic profile: blue profile represents the topography of gully alcove from alcove top to fan apex and red profile represents**  
 376 **the profile of gully fan from fan apex to fan toe.**

377

378

379 **Table 2.** Set of morphometric variables extracted from the studied gully systems and their formulas and/or description of  
 380 method.

Morphometric variable	Formula and/or description of method	References
Alcove length and width	Measured in km	<b>Tomczyk, 2021</b>
Alcove area	Measured in km <sup>2</sup>	<b>Tomczyk, 2021</b>
Fan length and width	Measured in km	<b>Tomczyk, 2021</b>
Fan area	Measured in km <sup>2</sup>	<b>Tomczyk, 2021</b>
Melton ratio	(Alcove relief)/(Alcove area <sup>0.5</sup> )	<b>Melton, 1957</b>
Relative concavity index (RCI)	Concavity Index/(maximum relief between the uppermost and lowermost points along the gully fan profile/2). Concavity Index is estimated as $\sum (H_i^* - H_i) / N$ , where $H_i^*$ is the elevation along the straight line, $H_i$ is the elevation along the gully fan profile, $N$ is the total number of measurement points.	<b>Langbein, 1964; Phillips and Lutz, 2008</b>
Alcove gradient	Measured in (°)	<b>Tomczyk, 2021</b>
Fan gradient	Measured in (°)	<b>Tomczyk, 2021</b>
Alcove relief	Measured in km	<b>Tomczyk, 2021</b>
Fan relief	Measured in km	<b>Tomczyk, 2021</b>
Relief ratio (alcove and fan)	Alcove/fan relief divided by the length of the alcove/fan	<b>Schumm, 1956a, b</b>
Alcove Perimeter	Measured in km	<b>Schumm, 1956a, b</b>
Form factor	Alcove area divided by the square of the length of the alcove	<b>Horton, 1932</b>
Elongation ratio	Diameter of a circle of the same area as the alcove divided by the maximum alcove length	<b>Schumm, 1956a, b</b>
Circularity ratio	Alcove area divided by the area of the circle having the same perimeter as the alcove perimeter	<b>Miller, 1953</b>

381

### 382 3.3 Gully system selection for morphometric measurements

383 We have selected only those gully systems for morphometric measurements in which: (i) the depositional fan from an alcove-  
 384 channel system is not superimposed by or interfingering with the fans from the neighboring channels, (ii) there is clear  
 385 association between the primary channel emanating from the alcove that extends downslope and then deposit its respective  
 386 fan, (iii) no evidence of extensive cross-cutting is seen with the neighboring channels on the walls, (iv) no evidence of extensive  
 387 mantling by dust/aeolian deposits is apparent, and (v) no evidence of channel/fan superposition on any topographic obstacle  
 388 on the walls or the floor of the crater is apparent, which may have influenced the morphometry. If in any case the fans

389 superimpose or channels cross-cut, we have carefully demarcated the alcove-channel-fan boundary, to minimize the  
390 inaccuracies in the measurements. Note that the selection of the gully systems was also constrained by the coverage of HiRISE  
391 DTMs used for morphometric analysis.

Deleted: that was

### 392 3.4 Statistical analysis of morphometric variables

393 We have two groups of gullies in our study: (1) gullies whose source areas are incised into LDM/glacial deposits and (2)  
394 gullies whose source areas are incised into the bedrock. First, for both the groups we have calculated descriptive statistics for  
395 each of the morphometric variables shown in Table 2. The significance of the difference between the values of each of the  
396 morphometric variables calculated for each group was tested using a Student's t-test. To apply t-tests, we have transformed  
397 the morphometric variables to remove skewness by taking their natural logarithm. Pearson correlation analysis has been used  
398 to investigate the correlation between the selected morphometric attributes of gully alcoves and fans. We infer strong positive  
399 correlations between variables if the correlation coefficient value is more than 0.7 and strong negative correlations if the value  
400 is less than -0.7. Very strong positive correlation between variables is inferred if the correlation coefficient is  $\geq 0.9$ . Further,  
401 we used canonical discriminant analysis (CDA) to determine morphometric variables that provide the most discrimination  
402 between the groups of gullies. In CDA, functions are generated according to the number of groups, until a number equal to n-  
403 1 functions is reached (n is the number of groups) (McLachlan, 2005). For the two groups of gullies in our study, there is going  
404 to be a function for which there is a standardised canonical discriminant function coefficient associated with the morphometric  
405 variable. The higher the magnitude of this coefficient for a particular morphometric variable, the higher the role of that variable  
406 in separating the groups of gullies (Conway et al., 2015). Standardisation was done by dividing each value for a given variable  
407 by the maximum value.

Deleted: is

Deleted: is

Deleted: Correlation

Deleted: (Conway et al., 2015)

## 408 4 Results

### 409 4.1 Morphology of gully systems

410 Out of the 29 gullied craters analysed in this work, we have found that there are 24 craters influenced by LDM and/or VFFs.  
411 The remaining 5 craters have gullies incised into the exposed underlying bedrock on the wall of the crater. Below we describe  
412 the substrates identified in the studied craters and then compare the morphology of the gullies formed into those substrates.

413 4 craters out of 24 craters (i.e. Raga, Roseau, unnamed crater in Newton basin and unnamed crater-1 in Terra Sirenum) have  
414 gullies that are only influenced by LDM. In these craters, we have found morphological evidence of LDM in the form of  
415 polygonized, smooth textured material on the pole-facing walls of the craters. Morphological evidence of VFF is not evident  
416 in these craters. In these craters, the gully-alcoves and gully channels appear to have been incised into the polygonized LDM  
417 material, and the gully-fan deposits are mantled. A typical example of this can be found in the unnamed crater formed inside  
418 the Newton basin (Fig. 4a). Roseau crater, in particular, contains a large number of gully systems whose alcoves and fans are

424 extensively mantled (Fig. 4b). The remaining 20 out of 24 craters contain evidence for gullies that are influenced by both LDM  
425 and glacial deposits (Table 1). The base of the pole-facing walls and the floor of the craters within which the gully systems  
426 have formed host linear-to-sinuuous arcuate ridges and VFFs, respectively. Typical examples of VFFs can be found in Corozal,  
427 Talu, unnamed craters in Terra Sirenum and Argyre basin, Langtang, Dechu and Dunkassa craters (Fig. 4c). In majority of the  
428 gullied craters (except Raga, Roseau and unnamed crater-1 in Terra Sirenum) influenced by LDM and glacial deposits, gully  
429 alcoves are found to have a distinctive V-shaped cross section in their mid-section (Figures 4d and 4e), they do not extend up

430 to the crater rim, and gully systems often show multiple episodes of activity, inferred by the presence of fresh channel incision  
431 on the gully-fan surfaces (Fig. 4d-e).

432 Istok, Galap, Gasa, Los, and an unnamed crater in the Terra Sirenum contain gully systems on the pole-facing walls that are  
433 not associated with LDM and VFFs (Table 1). The **gully** alcoves inside these craters have a crenulated shape and appear to  
434 have formed by headward erosion into the bedrock of the crater rim (Fig. 4f). These craters have formed large gully systems  
435 on their pole-facing walls, with brecciated alcoves, comprising of multiple sub-alcoves and hosting many clasts/boulders (Fig.  
436 4f).

437

438

439

440

441

442

443

444

445

446

447

448

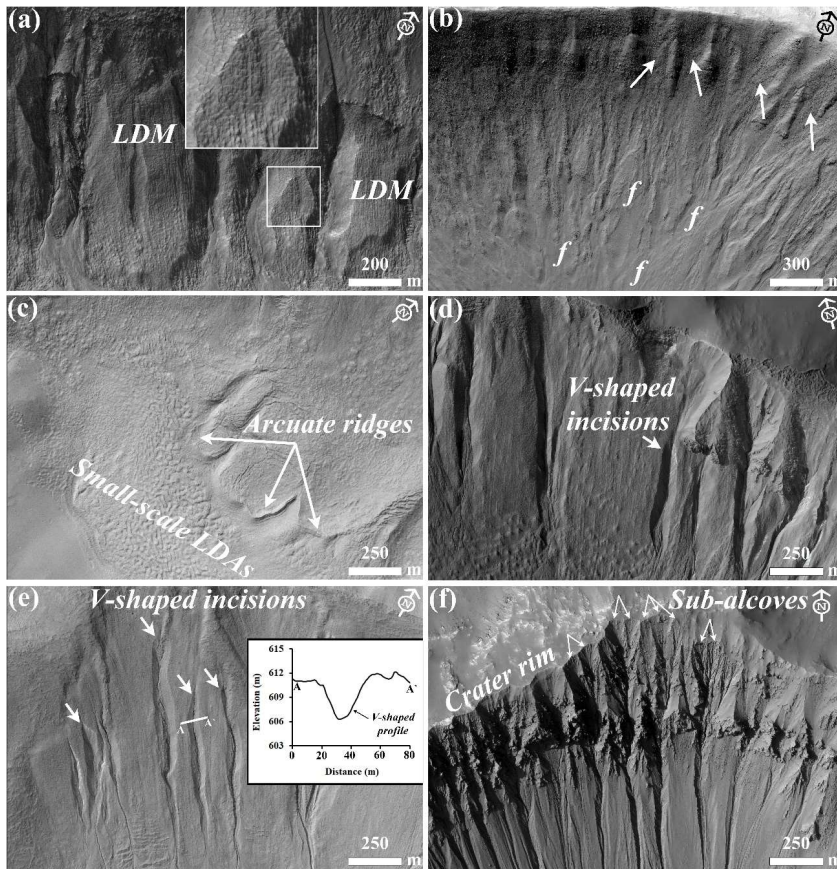
449

450

451

452

453



454 **Figure 4:** (a) LDM draped on the wall of an unnamed crater in the Newton basin. The inset shows details of the polygonal texture of  
455 the LDM. (HiRISE image PSP\_002686\_1410). (b) Infilled **gully** alcoves (arrows) and mantled fan surfaces (marked by letter 'f') on  
456 the wall of Roseau crater. (HiRISE image ESP\_024115\_1380). (c) Arcuate ridges at the foot of the crater wall and small-scale LDAs  
457 on the floor in Langtang crater. (HiRISE image ESP\_030099\_1415). (d) V-shaped incisions on the LDM draped walls of Taltal  
458 (HiRISE image ESP\_037074\_1400) and (e) Langtang crater (HiRISE image ESP\_030099\_1415). **Note the topographic profile (A-A)**  
459 **that illustrates V-shaped incision of the gully channel.** (f) **Gully** alcoves formed in Los crater by headward erosion into the crater  
460 rim. Individual **gully** alcoves formed in bedrock have multiple sub-alcoves. (HiRISE image ESP\_020774\_1445).

461

#### 462 4.2 Morphometry of gully systems

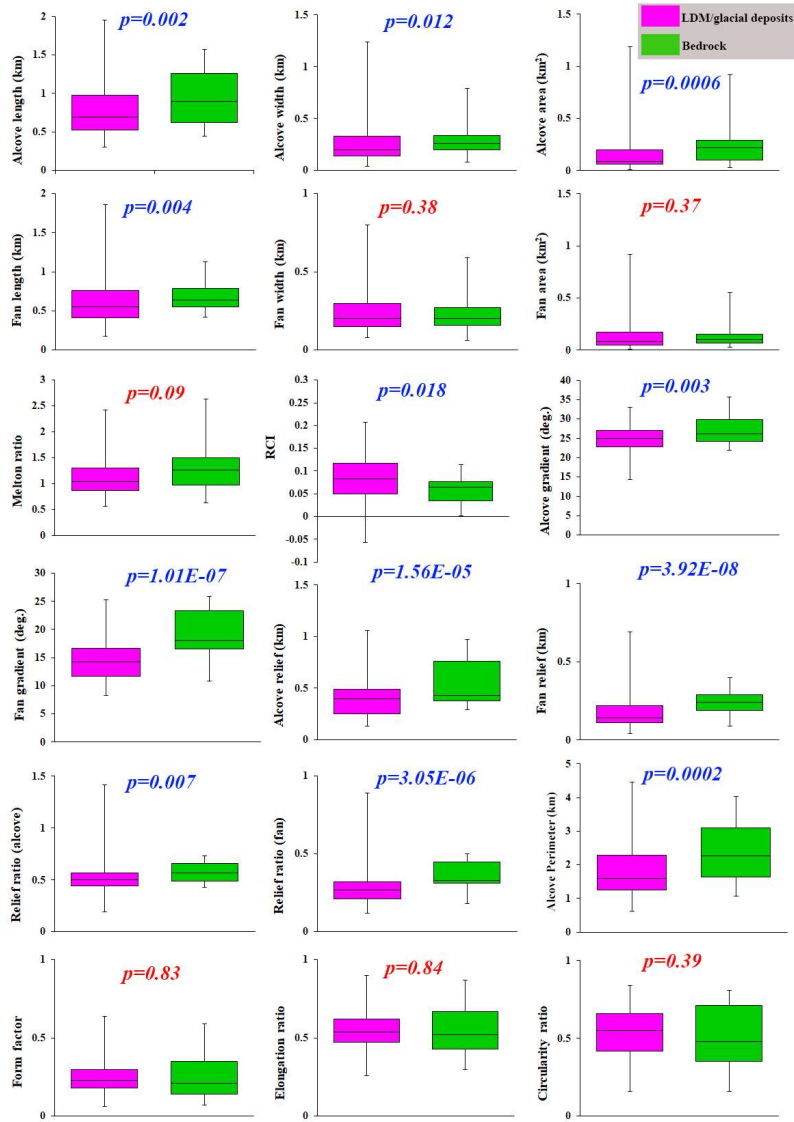
463 Based on the criteria summarized in section 3.3, we have studied 167 gullies across 29 craters for calculation of morphometric  
464 variables. 130 gullies are formed within LDM/glacial deposits, and 37 gullies are formed within the bedrock. The results of  
465 morphometric calculations are summarized for visual comparison as a boxplot (Fig. 5).

466 The results of the Student's t-test indicates that all of the morphometric variables in Table 2, except fan width, fan area, Melton  
467 ratio, form factor, elongation ratio, and circularity ratio, differ significantly between LDM/glacial deposits and bedrock (Fig.  
468 5). Compared to the mean gradient of gully-fans formed in LDM/glacial deposits, bedrock gully-fans are steeper and possess  
469 a higher relief ratio. The interquartile range of length, relief, and perimeter of **gully** alcoves formed in bedrock are also higher  
470 than the interquartile range of similar variables in LDM/glacial deposits, but the **gully** alcoves in LDM/glacial deposits possess  
471 much higher values of length, relief, and perimeter (Fig. 5).

472

Deleted: A

474  
475  
476  
477  
478  
479  
480  
481  
482  
483  
484  
485  
486  
487  
488  
489  
490  
491  
492  
493  
494  
495  
496  
497  
498  
499  
500  
501



502 **Figure 5: The boxplot presented here shows interquartile range, central horizontal bar shows median, and whiskers show range of**  
503 **values of alcove/fan geometry, relief, gradient, and dimensionless variables of gullies incised into LDM/glacial deposits (pink) and**  
504 **bedrock (green). P-values on the plots represent the results of the student's t-tests for testing the significance of difference in means**  
505 **of the morphometric variables between gully systems formed on LDM/Glacial deposits and bedrock. P-values in blue correspond to**  
506 **significant difference (with respect to a p-value of 0.05) and those in red are non-significant.**

507

508 **Pearson correlations** between morphometric attributes of **gully** alcoves and fans formed in bedrock and LDM/glacial deposits  
509 are summarized in Fig. 6. For bedrock, there are strong positive correlations between 12 pairs of morphometric variables and  
510 strong negative correlations between 3 pairs of morphometric variables. For LDM/glacial deposits, there are strong positive  
511 correlations between 18 pairs of morphometric variables and strong negative correlations between 3 pairs of morphometric  
512 variables. Very strong positive correlations (**>0.9**) are found between 9 pairs of morphometric variables for bedrock and  
513 between 4 pairs of morphometric variables for LDM/glacial deposits.

Deleted: Boxplots

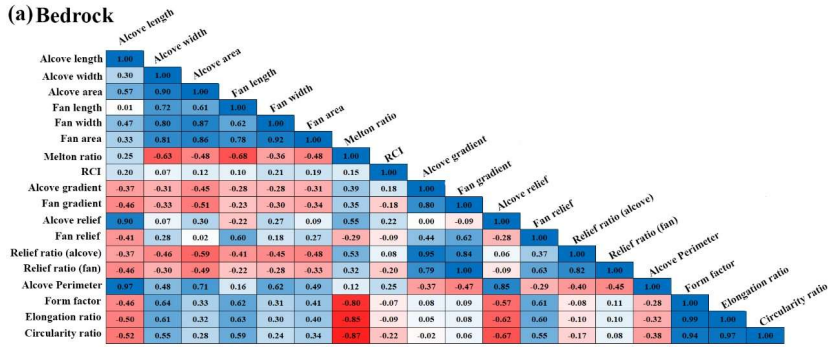
Deleted: showing the range of

Deleted: Correlations



517

(a) Bedrock



518

519

520

521

522

523

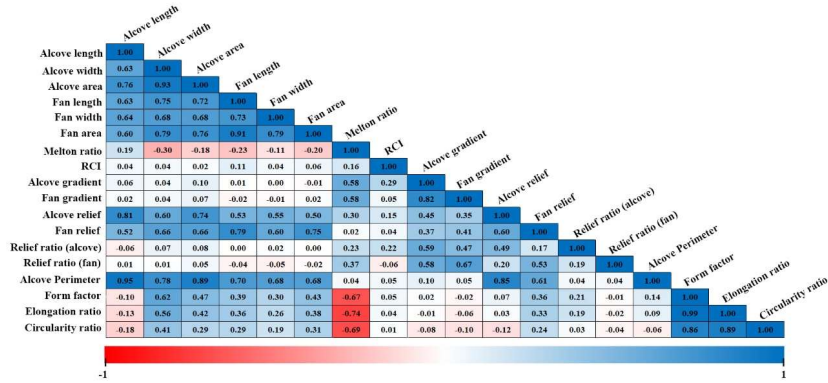
524

525

526

527

(b) LDM/glacial deposits



528

529

530

531

532

533

534

535

536

537

538

539 Figure 6: Pearson correlations between morphometric attributes of gully alcoves and fans formed in (a) bedrock and (b) LDM/glacial deposits. Values approaching either 1 or -1 have stronger correlations. Zero indicates no correlation.

541

542 The canonical discriminant analysis reveals that the following morphometric variables best distinguish between the gully systems formed in LDM/glacial deposits and bedrock, in descending order of importance: alcove perimeter, alcove relief, fan gradient, fan relief, fan length, relief ratio (alcove), alcove width, relief ratio (fan), alcove gradient, alcove area, alcove length, and relative concavity index (Table 3). The alcove perimeter is most important in discriminating among the gully systems formed within LDM/glacial deposits and bedrock, and the next two most important variables are alcove relief and fan gradient. Alcove relief and fan gradient have 4/5 and 1/3 the weight of alcove perimeter, respectively. Here, the weight values indicate

- Deleted: C
- Deleted: s
- Deleted: Higher the value of the correlation coefficient, higher is the strength of the correlation

552 the discriminator power in separating between the gullies formed in LDM/glacial deposits and bedrock. The remaining  
 553 variables such as fan relief, fan length, relief ratio (alcove), alcove width, and relief ratio (fan) have nearly 1/5 or greater (but  
 554 less than 1/3) of the weight of alcove perimeter discriminatory power in separating between the gullies formed in LDM/glacial  
 555 deposits and bedrock. The variables with the smallest magnitude, alcove gradient, alcove area, alcove length and relative  
 556 concavity index, have less than 1/10 the weight of the most important variable in separating the gully systems.

Deleted: the weight of alcove perimeter or greater

557 **Table 3.** Standardised canonical discriminant function coefficients (F1) that best separate gully systems formed on  
 558 LDM/Glacial deposits and bedrock.

Variable	F1
<u>Alcove</u> Perimeter	3.552
Alcove relief	-2.828
Fan gradient	1.278
Fan length	-1.06
Fan relief	1.06
Relief ratio (alcove)	0.971
Alcove width	-0.692
Relief ratio (fan)	-0.665
Alcove gradient	-0.331
Alcove area	-0.319
Alcove length	0.23
Relative concavity index	-0.182

559

560 **5 Discussion**

Deleted: s

561 **5.1 Unique morphology and morphometry of gully systems in different substrates**

562 We have found that the gully systems formed in LDM/glacial deposits and bedrock can, using discriminatory analysis, be  
 563 distinguished from one another in terms of perimeter and relief of gully alcoves (Table 3). Additionally, we have found  
 564 statistically significant difference between the perimeters and reliefs of gully alcoves formed in LDM/glacial deposits and  
 565 bedrock (Fig. 5). It is likely that these differences in the perimeters and reliefs of gully alcoves formed within morphologically  
 566 distinct substrates could be due to the integral nature of the surface material within which the gully alcoves have formed. In  
 567 other words, it is possible that the differences in the physical properties of the sediments (namely grain size, compactness etc.)  
 568 within which gully alcoves have formed played a key role in erosion of the substrate leading to differences in their

571 morphometric variables. Below we elaborate on the uniqueness of the substrates within which **gully** alcoves have formed, and  
572 discuss further the relationships between the morphometric variables of the morphologically distinct gully systems.

573 On Mars, VFFs contain high purity glacial ice with a debris cover (Sharp, 1973; Squyres, 1978, 1979; Squyres and Carr, 1986;  
574 Holt et al 2008, Plaut et al 2009, Petersen et al. 2018). Their surfaces have been interpreted to **comprise** of finer, reworked  
575 debris derived from sublimation of the underlying ice ([Baker et al., 2010](#); [Plaut et al., 2009](#)). The smooth, meters thick draping  
576 unit on the walls of formerly glaciated craters has been suggested to be derived from the atmosphere as a layer of dust-rich ice  
577 primarily constituting of fine-grained materials (Kreslavsky and Head, 2000; Mustard et al., 2001). The fine-grained materials  
578 are loosely-packed, unconsolidated materials exhibiting low thermal inertia values (Mellon et al., 2000; Putzig et al., 2005).  
579 Typically, gullies formed within this substrate display a smooth surface texture, wherein, evidence of individual clasts or  
580 meter-scale boulders is not resolvable in HiRISE images, substantiating the dominant component of fine-grained materials  
581 within the LDM (e.g., Levy et al., 2010; de Haas et al., 2015a). Additionally, it has been found that **gully** alcoves incised into  
582 the LDM always have a distinctive V-shaped cross section in their mid-section (Figures 4d and 4e), which when compared  
583 with similar-scaled systems on Earth also corresponds to the presence of loose sediments constituting the LDM (Conway et  
584 al., 2018). The **gully** alcoves with V-shaped cross sections are found to be elongated, likely indicating incision within ice-rich  
585 unlithified sediments (Aston et al., 2011). In the studied craters, we have found that gullies incised into LDM/glacial deposits  
586 **do have** an elongated, V-shaped cross section in their mid-sections (Fig. 4). We propose that the presence of fine-grained,  
587 loosely packed, unconsolidated materials within LDM/glacial deposits has facilitated formation of elongated **gully** alcoves  
588 with perimeters and reliefs relatively higher than that of **gully** alcoves formed in coarse-grained bedrock substrate. This is  
589 consistent with the previous studies suggesting that gullies eroding into LDM/glacial deposits have elongated catchments  
590 ([Aston et al., 2011](#)), whereas gullies eroding into the bedrock have more amphitheater-shaped catchments (Levy et al., 2009b).  
591 For this reason, the estimated length of **gully** alcoves formed in LDM/glacial deposits is found to be relative higher than that  
592 of **gully** alcoves formed in bedrock (Fig. 5). Furthermore, statistical analysis has revealed a significant difference between the  
593 length of **gully** alcoves formed in LDM/glacial deposits and bedrock (Fig. 5). Additionally, the presence of finer-grained  
594 sediments in LDM/glacial deposits is the likely cause of the V-shape of the incision of **gully** alcoves investigated in this study  
595 (Aston et al., 2011). On Earth, V-shaped incisions through glacial ice-rich moraines have been observed to have occurred  
596 during the paraglacial phase of glacial retreat (Bennett et al., 2000; Ewertowski and Tomczyk, 2015) (Fig. 7). The paraglacial  
597 phase refers to a terrestrial post-glacial period that represents the response of changing environment to deglaciation (Bennett  
598 et al., 2000; Ewertowski and Tomczyk, 2015).

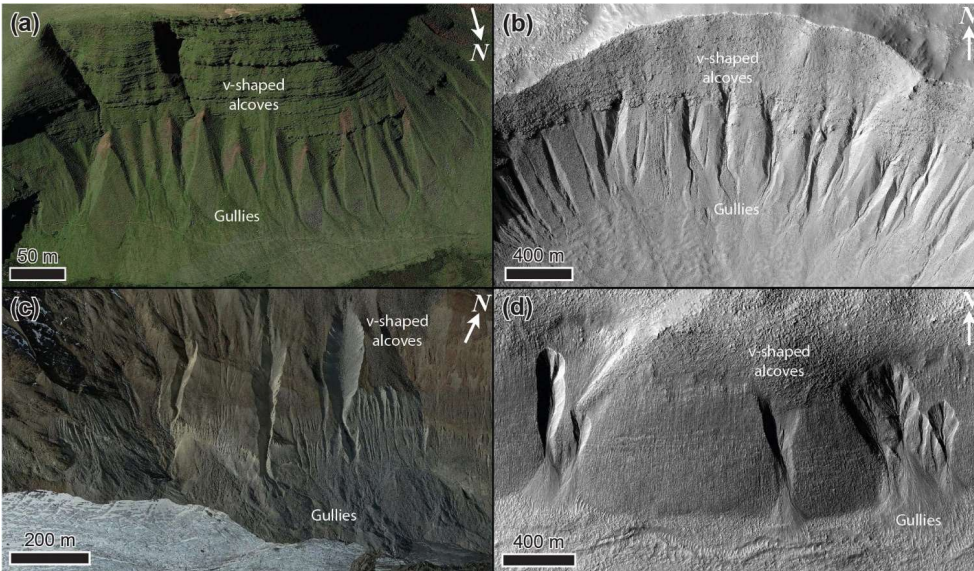
599

Deleted: be

Deleted: d

Deleted: Mangold, 2003; Levy et al., 2009a; Morgan et al., 2009

Deleted: are having



604

605 **Figure 7: Gullies forming in glacial sediments in deglaciated terrain in the (a) Brecon Beacons, Wales, UK on Earth (Google Earth**  
 606 **coordinates: 51°52'59.11"N, 3°43'33.26"W), (b) Talu crater ([https://www.uahirise.org/ESP\\_011817\\_1395](https://www.uahirise.org/ESP_011817_1395)) on Mars, (c)**  
 607 **Hintereisferner, Austria (Google Earth coordinates: 46°48'54.25"N, 10°47'8.18"E), on Earth, and (d) Bunnik crater**  
 608 **([https://www.uahirise.org/ESP\\_047044\\_1420](https://www.uahirise.org/ESP_047044_1420)) on Mars. HiRISE image credit: NASA/JPL-Caltech/University of Arizona.**

609

610 The next most important difference between these two types of gullies is the mean gradient of gully fans. At the foot of the  
 611 fans, mean gradient of the fans influenced by LDM/glacial deposits is  $<15^\circ$  for 61% of the studied fans. For bedrock, 84% of  
 612 the studied fans have a mean gradient  $>15^\circ$  at the foot of the fans. Hence, gully-fans formed in bedrock are emplaced at a  
 613 relatively steeper gradient than the fans formed from gullies in LDM/glacial deposits. We propose that the nature of the material  
 614 mobilized can explain this difference, with the finer-grained sediments characteristic of the LDM/glacial type gullies being  
 615 easier to mobilise and being entrained to lower slope angles, than the coarser sediments found within the bedrock type gullies.

## 616 5.2 Evaluation of the gully formation process

617 On Earth, alcove-fan systems can roughly be subdivided in flood-dominated, debris-flow dominated, and colluvial systems.  
 618 Following the terminology of De Haas et al., (2015b) and Tomczyk (2021), we define these systems as follows:

619 1) Flood-dominated systems: These are systems dominated by fluid-gravity flows, i.e., water floods, hyperconcentrated floods,  
620 and debris floods. The fans of such systems are commonly referred to as fluvial or alluvial fans (e.g., Ryder, 1971; Blair and  
621 McPherson, 1994; Hartley et al., 2005).

622 2) Debris-flow dominated systems: These are systems dominated by sediment-gravity flows, i.e., debris flows, mud flows.  
623 Irrespective of their radial extent and depositional gradients, the fans aggraded by these systems can be commonly called  
624 debris-flow fans or debris fans (Blikra and Nemeč, 1998; de Scally et al., 2010).

625 3) Colluvial systems: These are systems dominated by rock-gravity and sediment-gravity flows, with their dominant activity  
626 relating to rockfalls, grain flows, and snow avalanches (in periglacial and alpine settings). Debris flows typically constitute  
627 only a relatively minor component of geomorphic processes in such systems. The fans of these systems are also commonly  
628 known as colluvial cones or talus cones (Siewert et al., 2012; De Haas et al., 2015b).

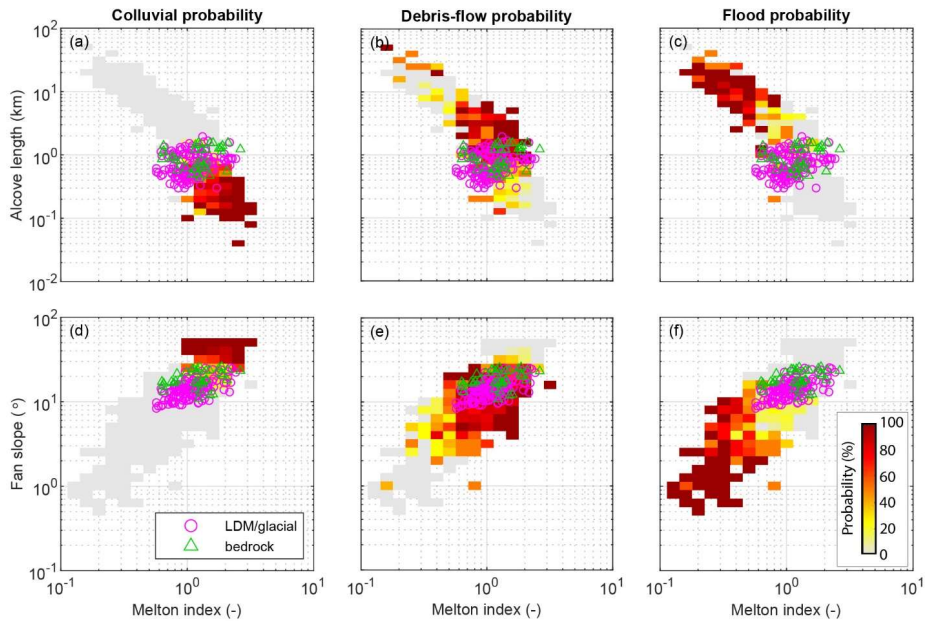
629 Although these systems may be dominated by one type of geomorphic process, it is important to stress that other processes  
630 may also occur. For example, on Earth water floods are not uncommon on many debris-flow dominated systems, while debris-  
631 flow deposits are commonly recognized on colluvial cones.

632

633

634

635



636

637 **Figure 8: Comparison of combinations of Melton ratio with Alcove length and Fan gradient. The probability heat maps**  
638 **are based on previously published data – see text for references. The Martian gully systems formed in LDM/glacial**  
639 **deposits and bedrock are found to be in the debris-flow regime on Earth. The gray area shows the realm of the colluvial,**  
640 **debris-flow, and fluvial fans together.**

641

642 To compare the morphometric characteristics of the Martian gully systems to terrestrial systems, we have compiled  
643 morphometric data of gully alcoves and fans across several continents, mountain ranges, climate zones, and process types on  
644 Earth. This dataset includes published data from the Himalayas, Ladakh, India (Stolle et al., 2013), the tropical Andes,  
645 Columbia (Arango et al., 2021), Spitsbergen, Svalbard (Tomczyk, 2021), British Columbia, Canada (Kostaschuk, 1986;  
646 Jackson et al., 1987; and newly presented data), the southern Carpathians, Romania (Ilinca et al., 2021), the Southern Alps,  
647 New Zealand (De Scally and Owens, 2004; De Scally et al., 2010), the North Cascade Foothills, USA, the European Alps  
648 (including Switzerland, Italy, France, and Austria), and the Pyrenees (from multiple authors compiled by Bertrand et al., 2013).  
649 The dataset comprises information from colluvial, debris-flow, and flood (also including debris flood) dominated systems. In

650 total, it contains 231 colluvial systems, 749 debris-flow dominated systems, and 369 flood-dominated systems. In total, data  
651 were compiled for 1349 systems, although not all information was available for all systems, with data availability ranging from  
652 729 sites for alcove length to all 1349 systems for Melton index and process type. Based on this data we have made a heatmap  
653 of the probability of flood, debris-flow, or colluvially-dominated conditions for combinations of Melton ratio with alcove  
654 length and fan gradient, to which we compare the Martian gullies (Fig. 8). We have specifically chosen the combinations of  
655 Melton ratio with alcove length and fan gradient to infer the Martian gully formative mechanism because they have been  
656 widely used in discriminating terrestrial drainage basins and fans prone to flooding from those subject to debris flows, debris  
657 floods and floods (e.g. De Scally and Owens, 2004; Wilford et al., 2004). We have found that the Martian gullies are indeed  
658 in the debris-flow regime on Earth. Moreover, they are closer to the transition to the smaller and steeper colluvial cones than  
659 to transition to flood-dominated fans. As expected, bedrock systems in Fig. 8d-e are closer to the colluvial systems than the  
660 LDM systems.

661

662 According to the previous reports of debris-flow like deposits found in Martian gullies (e.g. Johnsson et al., 2014; Sinha et al.,  
663 2019, 2020), the morphological attributes of debris-flow like deposits typically include overlapping tongue-shaped lobes with  
664 embedded clasts, channels with medial deposits, and channels with clearly defined lateral levees. Although it is still not clear  
665 whether the formation of these deposits in gullies are from sublimation of CO<sub>2</sub> ice or due to meltwater generation. De Haas et  
666 al., (2019b) showed that CO<sub>2</sub> sublimation may lead to flow fluidization on Mars in a manner similar to fluidization by water  
667 in terrestrial debris flows; a concept supported by the recent finding of lobate deposits and boulder-rich levee formation during  
668 the present-day in Istok crater (Table 1) (Dundas et al., 2019). The formation of these morphologically similar deposits during  
669 the present-day is attributed to sublimating CO<sub>2</sub> frost, which likely produces the necessary fluidization likely by gas generated  
670 from entrained CO<sub>2</sub> frost (Dundas et al., 2019). On the basis of these recent reports (De Haas et al., 2019b; Dundas et al., 2019)  
671 and based on our own findings in this study, we argue that a debris-flow like process similar to those operated in the terrestrial  
672 gully systems has likely dominated the flow types that lead to gully formation on Mars. Present-day sublimation of CO<sub>2</sub> ice  
673 on Mars may have provided the necessary flow fluidization for the emplacement of deposits similar to terrestrial debris-flow  
674 like deposits (De Haas et al., 2019b).

## 675 6 Conclusions

676 This paper compares morphological and morphometric characteristics of gully alcoves and associated fans formed in  
677 LDM/glacial deposits and bedrock over walls of 29 craters between 30° S and 75° S latitudes on Mars. 5 craters out of 29 have  
678 alcoves-fans formed within the bedrock and remaining 24 craters have alcoves-fans formed within LDM/glacial deposits. From  
679 our analysis of 167 gullies, we posit that gully systems formed in LDM/glacial deposits and bedrock differ from one another  
680 using the following lines of evidence:

**Formatted:** Subscript

**Deleted:** It is likely that the present-day sublimation of CO<sub>2</sub> ice on Mars provided

683 • Gully alcoves formed in LDM/glacial deposits are more elongated than the gully alcoves formed in bedrock, and possess a  
684 distinctive V-shaped cross section.

Deleted: A

685 • The mean gradient of gully-fans formed in bedrock is steeper than the mean gradient of fans formed from gullies in  
686 LDM/glacial deposits.

687 The morphological distinction reported between gullies formed in the bedrock and LDM/glacial deposits signifies that Martian  
688 gullies may have multiple formative environments. We infer that the presence of mantling material could be one of the key  
689 factors in constraining the mechanisms forming Martian gully systems and that presence of LDM would promote formation  
690 of elongated gully alcoves with perimeters and reliefs relatively higher than that of gully alcoves formed in coarse-grained  
691 bedrock substrate.

Deleted: mechanisms

692 Based on the combinations of Melton ratio with alcove length and fan gradient, we suggest that the gully systems studied in  
693 this work were likely dominated by terrestrial debris-flow like processes during their formation. This is consistent with the  
694 findings reported in previous studies that showed evidence of formation of deposits morphologically similar to terrestrial  
695 debris-flow like deposits, both in the past and during the present-day (e.g., Johnsson et al., 2014; Dundas et al., 2019). The  
696 present-day sublimation of CO<sub>2</sub> ice on Mars is envisaged to provide the necessary flow fluidization for the emplacement of  
697 deposits similar to debris-flow like deposits on Earth (De Haas et al., 2019b).

#### 698 7 Author contribution

699 RKS, TDH and SJC conceptualized this work. The methodology was developed by RKS, TDH and SJC. Data curation and  
700 formal analyses were performed by RKS. TDH and AN also contributed in collection of datasets used in this work. RKS, DR,  
701 TDH and SJC contributed to the interpretation of the data and results. RKS wrote the original draft of this paper, which was  
702 reviewed and edited by all authors.

#### 703 8 Conflict of interest

704 SJC is a Guest Editor of this special issue (Planetary landscapes, landforms, and their analogues) of ESurf and on the editorial  
705 board for ESurf. The peer-review process was guided by an independent editor, and the authors have also no other competing  
706 interests to declare.

Deleted: D

#### 707 9 Acknowledgements

708 We are grateful and thank both the anonymous reviewers for thorough assessment of our manuscript and for providing us  
709 constructive comments and suggestions. Thanks to the Editor (Heather Viles) and Associate Editor (Frances E. G. Butcher) at  
710 Earth Surface Dynamics for the editorial handling of the manuscript. We would like to thank the HiRISE team for their work  
711 to produce the images and digital elevation models used in this study, it would have been impossible without them. RKS and



715 DR acknowledge the financial support by the Indian Space Research Organisation, Department of Space, Government of India.  
716 SJC and AN are grateful for the financial support from Région Pays de la Loire, project étoiles montantes METAFLOWS  
717 (convention N° 2019-14294) and also the financial support of CNES in support of their HiRISE work. TdH was supported by  
718 the Netherlands Organisation for Scientific Research (NWO) (grant 016.Veni.192.001). We acknowledge the efforts of team  
719 MUTED to develop an online tool (<http://muted.wwu.de/>) for quick identification of the spatial and multi-temporal coverage  
720 of planetary image data from Mars. All the planetary datasets used in this work are available for free download at the PDS  
721 Geosciences Node Mars Orbital Data Explorer (ODE) (<https://ode.rsl.wustl.edu/mars/>) and <https://www.uahirise.org/>. The  
722 newly-generated DTMs can be downloaded from [https://figshare.com/articles/dataset/Self\\_generated\\_DEMs/21717164](https://figshare.com/articles/dataset/Self_generated_DEMs/21717164).  
723 The measurement datasets can be downloaded from  
724 [https://figshare.com/articles/dataset/Measurement\\_data\\_of\\_gully\\_systems\\_in\\_the\\_southern\\_mid\\_latitudes\\_of\\_Mars/](https://figshare.com/articles/dataset/Measurement_data_of_gully_systems_in_the_southern_mid_latitudes_of_Mars/21717182)  
725 [21717182](https://figshare.com/articles/dataset/Measurement_data_of_gully_systems_in_the_southern_mid_latitudes_of_Mars/21717182). This work is a part of the PhD work of Rishitosh K. Sinha. Director PRL, Head of Planetary Science Division,  
726 PRL, Head of Planetary Remote Sensing Section, PRL, and Director IIT Gandhinagar are gratefully acknowledged for constant  
727 encouragement during the work.

## 728 References

- 729 Arango, M. I., Aristizábal, E., & Gómez, F.: Morphometrical analysis of torrential flows-prone catchments in tropical and  
730 mountainous terrain of the Colombian Andes by machine learning techniques, *Natural Hazards*, 105(1), 983-1012, doi:  
731 <https://doi.org/10.1007/s11069-020-04346-5>, 2021.
- 732 Arfstrom, J. & Hartmann, W.K.: Martian flow features, moraine-like ridges, and gullies: terrestrial analogs and  
733 interrelationships, *Icarus*, 174, 321–335, doi: <https://doi.org/10.1016/j.icarus.2004.05.026>, 2005.
- 734 Aston, A., Conway, S. & Balme, M.: Identifying Martian Gully Evolution. In: Balme, M.R., Bargery, A.S., Gallagher, C.J. &  
735 Gupta, S. (eds) *Martian Geomorphology*, Geological Society, London, Special Publications, 356, 151–169, doi:  
736 <https://doi.org/10.1144/SP356.9>, 2011.
- 737 [Baker, D. M. H., James W. H., and David R. M.: Flow patterns of lobate debris aprons and lineated valley fill north of Ismeniae](#)  
738 [Fossae, Mars: Evidence for extensive mid-latitude glaciation in the Late Amazonian, \*Icarus\* 207, 186-209, 2010, doi:](#)  
739 <https://doi.org/10.1016/j.icarus.2009.11.017>.
- 740 Balme, M., Mangold, N. Et Al.: Orientation and distribution of recent gullies in the southern hemisphere of Mars: observations  
741 from High Resolution Stereo Camera/Mars Express (HRSC/MEX) and Mars Orbiter Camera/Mars Global Surveyor  
742 (MOC/MGS) data, *J. Geophys. Res.: Planets*, 111, E05001, doi: <https://doi.org/10.1029/2005JE002607>, 2006.
- 743 Bertrand, M., Liébault, F., & Piégay, H.: Debris-flow susceptibility of upland catchments, *Natural Hazards*, 67(2), 497-511,  
744 doi: <https://doi.org/10.1007/s11069-013-0575-4>, 2013.

745 Blair, T.C. & McPherson, J.G.: Processes and forms of alluvial fans. In: PARSONS, A. & ABRAHAMS, A. (eds)  
746 Geomorphology of Desert Environments, Springer, Dordrecht, The Netherlands, 413–467, doi: [https://doi.org/10.1007/978-1-](https://doi.org/10.1007/978-1-4020-5719-9_14)  
747 [4020-5719-9\\_14](https://doi.org/10.1007/978-1-4020-5719-9_14), 2009.

748 Blair, T.C.: Sedimentology of the debris-flow-dominated Warm Spring Canyon alluvial fan, Death Valley, California,  
749 Sedimentology 46 (5), 941–965, doi: <https://doi.org/10.1046/j.1365-3091.1999.00260.x>, 1999.

750 Blikra, L.H., Nemeč, W.: Postglacial colluvium in western Norway: depositional processes, facies and palaeoclimatic record.  
751 Sedimentology 45 (5), 909–960, doi: <https://doi.org/10.1046/j.1365-3091.1998.00200.x>, 1998.

752 Cedillo-Flores, Y., Treiman, A.H., Lasue, J. & Clifford, S.M.: CO<sub>2</sub> gas fluidization in the initiation and formation of Martian  
753 polar gullies, Geophys. Res. Letters, 38, L21202 doi: <https://doi.org/10.1029/2011GL049403>, 2011.

754 Christensen, P.R.: Formation of recent Martian gullies through melting of extensive water-rich snow deposits, Nature, 422,  
755 45–48, doi: <https://doi.org/10.1038/nature01436>, 2003.

756 Conway, S. J., Butcher, F. E., de Haas, T., Deijns, A. A., Grindrod, P. M., & Davis, J. M.: Glacial and gully erosion on Mars:  
757 A terrestrial perspective, Geomorphology, 318, 26–57, doi: <https://doi.org/10.1016/j.geomorph.2018.05.019>, 2018.

758 Conway, S.J. & Balme, M.R.: Decameter thick remnant glacial ice deposits on Mars, Geophys. Res. Letters, 41, 5402–5409,  
759 doi: <https://doi.org/10.1002/2014GL060314>, 2014.

760 Conway, S.J., Balme, M.R., Kreslavsky, M.A., Murray, J.B. & Towner, M.C.: The comparison of topographic long profiles  
761 of gullies on Earth to gullies on Mars: a signal of water on Mars. Icarus, 253, 189–204, doi:  
762 <https://doi.org/10.1016/j.icarus.2015.03.009>, 2015.

763 Conway, S.J., Balme, M.R., Murray, J.B., Towner, M.C., Okubo, C.H. & Grindrod, P.M.: The indication of Martian gully  
764 formation processes by slope–area analysis, In: Balme, M.R., Bargery, A.S., Gallagher, C.J. & Gupta, S. (eds) Martian  
765 Geomorphology, Geological Society, London, Special Publications, 356, 171–201, doi: <https://doi.org/10.1144/SP356.10>,  
766 2011.

767 Conway, S.J., Harrison, T.N., Soare, R.J., Britton, A.W. & Steele, L.J.: New slope-normalized global gully density and  
768 orientation maps for Mars, In: Conway, S.J., Carrivick, J.L., Carling, P.A., De Haas, T. & Harrison, T.N. (eds) Martian Gullies  
769 and their Earth Analogues, Geol. Soc. Lond. Spec. Publ. 467. First published online November 27, 2017, doi:  
770 <https://doi.org/10.1144/SP467.3>, 2017.

771 Costard, F., Forget, F., Mangold, N. & Peulvast, J.P.: Formation of recent Martian debris flows by melting of near-surface  
772 ground ice at high obliquity, Science, 295, 110–113, doi: [10.1126/science.1066](https://doi.org/10.1126/science.1066), 2002.

773 Crosta, G.B., Frattini, P.: Controls on modern alluvial fan processes in the central Alps, northern Italy, *Earth Surf. Proc. Land*.  
774 29 (3), 267–293, doi: <https://doi.org/10.1002/esp.1009>, 2004.

775 de Haas, T., Conway, S.J., Butcher, F.E.G., Levy, J.S., Grindrod, P.M., Balme, M.R., Goudge, T.A.: Time will tell: temporal  
776 evolution of Martian gullies and paleoclimatic implications, *Geol. Soc. Lond. Spec. Publ.* 467, doi:  
777 <https://doi.org/10.1144/SP467.1>, 2019a.

778 de Haas, T., McArdell, B. W., Conway, S. J., McElwaine, J. N., Kleinhans, M. G., Salese, F., & Grindrod, P. M.: Initiation  
779 and flow conditions of contemporary flows in Martian gullies, *J. Geophys. Res.: Planets*, 124(8), 2246-2271, doi:  
780 <https://doi.org/10.1029/2018JE005899>, 2019b.

781 de Haas, T., Hauber, E. & Kleinhans, M.G. 2013. Local late Amazonian boulder breakdown and denudation rate on Mars,  
782 *Geophys. Res. Letters*, 40, 3527–3531, doi: <https://doi.org/10.1002/grl.50726>, 2013.

783 de Haas, T., Ventra, D., Hauber, E., Conway, S.J. & Kleinhans, M.G.: Sedimentological analyses of Martian gullies: the  
784 subsurface as the key to the surface, *Icarus*, 258, 92–108, doi: <https://doi.org/10.1016/j.icarus.2015.06.017>, 2015a.

785 de Haas, T., Kleinhans, M. G., Carbonneau, P. E., Rubensdotter, L., & Hauber, E.: Surface morphology of fans in the high-  
786 Arctic periglacial environment of Svalbard: Controls and processes, *Earth-Science Reviews*, 146, 163-182, doi:  
787 <https://doi.org/10.1016/j.earscirev.2015.04.004>, 2015b.

788 de Scally, F. A., & Owens, I. F.: Morphometric controls and geomorphic responses on fans in the Southern Alps, New Zealand,  
789 *Earth Surface Processes and Landforms: The Journal of the British Geomorphological Research Group*, 29(3), 311-322, doi:  
790 <https://doi.org/10.1002/esp.1022>, 2004.

791 De Scally, F.A., Owens, I.F., Louis, J.: Controls on fan depositional processes in the schist ranges of the Southern Alps, New  
792 Zealand, and implications for debris-flow hazard assessment, *Geomorphology* 122 (1–2), 99–116, doi:  
793 <https://doi.org/10.1016/j.geomorph.2010.06.002>, 2010.

794 Dickson, J.L. & Head, J.W.: The formation and evolution of youthful gullies on Mars: gullies as the latestage phase of Mars  
795 most recent ice age, *Icarus*, 204, 63–86, doi: <https://doi.org/10.1016/j.icarus.2009.06.018>, 2009.

796 Dickson, J.L. et al.: Recent climate cycles on Mars: Stratigraphic relationships between multiple generations of gullies and the  
797 latitude dependent mantle, *Icarus* 252, 83–94, doi: <http://dx.doi.org/10.1016/j.icarus.2014.12.035>, 2015.

798 Dickson, J.L., Head, J.W., Fassett, C.I.: Patterns of accumulation and flow of ice in the mid-latitudes of Mars during the  
799 Amazonian, *Icarus* 219, 723–732, doi: <http://dx.doi.org/10.1016/j.icarus.2012.03.010>, 2012.

800 Dickson, J.L., Head, J.W., Kreslavsky, M.: Martian gullies in the southern midlatitudes of Mars: Evidence for climate-  
801 controlled formation of young fluvial features based upon local and global topography, *Icarus* 188, 315–323, doi:  
802 <https://doi.org/10.1016/j.icarus.2006.11.020>, 2007.

803 Dundas, C. M., McEwen, A. S., Diniega, S., Hansen, C. J., Byrne, S., & McElwaine, J. N.: The formation of gullies on Mars  
804 today, *Geol. Soc. Lond. Spec. Publ.* 467, 67-94, doi: <https://doi.org/10.1144/SP46>, 2019.

805 Dundas, C.M., Diniega, S., Hansen, C.J., Byrne, S., McEwen, A.S.: Seasonal activity and morphological changes in martian  
806 gullies, *Icarus* 220:124–143, doi: <https://doi.org/10.1016/j.icarus.2012.04.005>, 2012.

807 Dundas, C.M., Diniega, S., McEwen, A.S.: Long-term monitoring of Martian gully formation and evolution with  
808 MRO/HiRISE, *Icarus* 251:244–263, doi: <https://doi.org/10.1016/j.icarus.2014.05.013>, 2015.

809 Hargitai, H. (2014). Viscous Flow Features (Mars). In: *Encyclopedia of Planetary Landforms*. Springer, New York, NY.  
810 [https://doi.org/10.1007/978-1-4614-9213-9\\_596-1](https://doi.org/10.1007/978-1-4614-9213-9_596-1)

811 Harrison, T.N., Osinski, G.R., Tornabene, L.L., Jones, E.: Global documentation of gullies with the Mars reconnaissance  
812 orbiter context camera and implications for their formation, *Icarus* 252:236–254, doi:  
813 <https://doi.org/10.1016/j.icarus.2015.01.022>, 2015.

814 Hartley, A.J., Mather, A.E., Jolley, E., Turner, P.: Climatic controls on alluvial-fan activity, Coastal Cordillera, northern Chile.  
815 In: Harvey, A.M., Mather, A.E., Stokes, M. (Eds.), *Alluvial Fans: Geomorphology, Sedimentology, Dynamics*. *Geol. Soc.*  
816 *Lond. Spec. Publ.* 251, 95-115, doi: <https://doi.org/10.1144/GSL.SP.2005.251.01>, 2005.

817 Head, J.W., Marchant, D.R., Dickson, J.L., Kress, A.M., Baker, D.M.: Northern midlatitude glaciation in the Late Amazonian  
818 period of Mars: criteria for the recognition of debris-covered glacier and valley glacier landsystem deposits, *Earth Planet. Sci.*  
819 *Lett.* 294:306–320, doi: <https://doi.org/10.1016/j.epsl.2009.06.041>, 2010.

820 HELDMANN, J.L. & MELLON, M.T.: Observations of Martian gullies and constraints on potential formation mechanisms,  
821 *Icarus*, 168, 285–304, doi: <https://doi.org/10.1016/j.icarus.2003.11.024>, 2004.

822 Heldmann, J.L. et al.: Formation of martian gullies by the action of liquid water flowing under current martian environmental  
823 conditions, *J. Geophys. Res. Planets* 110, doi: <http://dx.doi.org/10.1029/2004JE002261>, 2005.

824 Hobbs, S.W., Paull, D.J., Clark, J.D.A.: A comparison of semiarid and subhumid terrestrial gullies with gullies on Mars:  
825 Implications for martian gully erosion, *Geomorphology* 204, 344–365, doi: <http://dx.doi.org/10.1016/j.geomorph.2013.08.018>,  
826 2014.

827 Hobbs, S.W., Paull, D.J. and Clarke, J.D.A.: Analysis of regional gullies within Noachis Terra, Mars: A complex relationship  
828 between slope, surface material and aspect, *Icarus*, 250, 308-331, doi: <https://doi.org/10.1016/j.icarus.2014.12.011>, 2015.

829 Hubbard, B., Milliken, R.E., Kargel, J.S., Limaye, A. & Souness, C.: Geomorphological characterisation and interpretation of  
830 a mid-latitude glacier-like form: Hellas Planitia, Mars, *Icarus*, 211, 330–346, doi: <https://doi.org/10.1016/j.icarus.2010.10.021>,  
831 2011.

832 Ilinca, V.: Using morphometrics to distinguish between debris flow, debris flood and flood (Southern Carpathians, Romania),  
833 *Catena*, 197, 104982, doi: <https://doi.org/10.1016/j.catena.2020.104982>, 2021.

834 Jackson LE, Kostaschuk RA, MacDonald GM: Identification of debris flow hazard on alluvial fans in the Canadian Rocky  
835 Mountains, In: Costa JE, Wieczorek GF (eds) *Debris flows/avalanches: process, recognition, and mitigation*. *Rev Eng Geol*  
836 vol. VII. *Geol. Soc. Am*, doi: <https://doi.org/10.1130/REG7-p115>, 1987.

837 Johnsson, A. et al.: Evidence for very recent melt-water and debris flow activity in gullies in a young mid-latitude crater on  
838 Mars, *Icarus* 235, 37–54, doi: <http://dx.doi.org/10.1016/j.icarus.2014.03.005>, 2014.

839 Kirk, R.L., Howington-Kraus, E., Rosiek, M.R., Anderson, J.A., Archinal, B.A., Becker, K.J., Cook, D.A., Galuszka, D.M.,  
840 Geissler, P.E., Hare, T.M., Holmberg, I.M., Keszthelyi, L.P., Redding, B.L., Delamere, W.A., Gallagher, D., Chapel, J.D.,  
841 Eliason, E.M., King, R., McEwen, A.S.: Ultrahigh resolution topographic mapping of Mars with MRO HiRISE stereo images:  
842 meter-scale slopes of candidate Phoenix landing sites, *J. Geophys. Res. Planets* 113, doi:  
843 <https://doi.org/10.1029/2007JE003000>, 2008.

844 Kostaschuk, R.A., Macdonald, G.M., Putnam, P.E.: Depositional process and alluvial fan-drainage basin morphometric  
845 relationships near Banff, Alberta, Canada, *Earth Surf. Proc. Land*. 11 (5), 471–484, doi:  
846 <https://doi.org/10.1002/esp.3290110502>, 1986.

847 Kreslavsky, M.A.: Slope steepness of channels and aprons: Implications for origin of martian gullies. Workshop Martian  
848 Gullies, Workshop on Martian Gullies 2008. Abs.#1301, 2008.

849 Kreslavsky, M.A., Head, J.W.: Mars: nature and evolution of young latitudedependent water-ice-rich mantle, *Geophys. Res.*  
850 *Lett.* 29, doi: <https://doi.org/10.1029/2002GL015392>, 2002.

851 Langbein, W. B.: Profiles of rivers of uniform discharge, *U.S. Geol. Surv. Prof. Pap.*, 501-B, 119– 122, doi:  
852 <https://doi.org/10.1086/627653>, 1964.

853 Lanza, N. L., Meyer, G. A., Okubo, C. H., Newsom, H. E., & Wiens, R. C.: Evidence for debris flow gully formation initiated  
854 by shallow subsurface water on Mars, *Icarus*, 205(1), 103-112, doi: <https://doi.org/10.1016/j.icarus.2009.04.014>, 2010.

855 Levy, J.S. et al.: Identification of gully debris flow deposits in Protonilus Mensae, Mars: Characterization of a water-bearing,  
856 energetic gully-forming process, *Earth Planet. Sci. Lett. Mars Express after 6 Years in Orbit: Mars Geology from Three-*  
857 *Dimensional Mapping by the High Resolution Stereo Camera (HRSC) Experiment* 294, 368–377, doi:  
858 <https://doi.org/10.1016/j.epsl.2009.08.002>, 2010b.

859 Levy, J.S., Head, J., Marchant, D.: Thermal contraction crack polygons on Mars: classification, distribution, and climate  
860 implications from HiRISE observations, *J. Geophys. Res. Planets* 114, 01007, doi: <https://doi.org/10.1029/2008JE003273>,  
861 2009a.

862 Levy, J. S., Head, J. W., Marchant, D. R., Dickson, J. L., & Morgan, G. A.: Geologically recent gully–polygon relationships  
863 on Mars: Insights from the Antarctic Dry Valleys on the roles of permafrost, microclimates, and water sources for surface  
864 flow, *Icarus*, 201(1), 113-126, doi: <https://doi.org/10.1016/j.icarus.2008.12.043>, 2009b.

865 Levy, J.S., Head, J.W., Marchant, D.R.: Gullies, polygons and mantles in Martian permafrost environments: cold desert  
866 landforms and sedimentary processes during recent Martian geological history, *Geol. Soc. Lond. Spec. Publ.* 354, 167–182,  
867 doi: <https://doi.org/10.1144/SP354.10>, 2011.

868 Malin, M.C., Edgett, K.S.: Evidence for recent groundwater seepage and surface runoff on Mars. *Science* 288:2330–2335, doi:  
869 <https://doi.org/10.1126/science.288.5475.2330>, 2000.

870 McEwen, A.S., Eliason, E.M. et al.: Mars reconnaissance orbiter’s High Resolution Imaging Science Experiment (HiRISE), *J.*  
871 *Geophys. Res.: Planets*, 112, E05S02, doi: <https://doi.org/10.1029/2005JE002605>, 2007.

872 [McLachlan, G. J.: Discriminant analysis and statistical pattern recognition, John Wiley & Sons, 2005.](#)

873 Melton, M.A.: An analysis of the relation among elements of climate, surface properties and geomorphology, Office of Nav.  
874 Res. Dept. Geol. Columbia Univ, NY. Tech. Rep. 11, 1975.

875 Milliken, R.E., Mustard, J.F., Goldsby, D.L.: Viscous flow features on the surface of Mars: observations from high-resolution  
876 Mars Orbiter Camera (MOC) images, *J. Geophys. Res.* 108, doi: <https://doi.org/10.1029/2002JE002005>, 2003.

877 Mustard, J.F., Cooper, C.D., Rifkin, M.K.: Evidence for recent climate change on Mars from the identification of youthful  
878 near-surface ground ice, *Nature* 412:411–414, doi: <https://doi.org/10.1038/35086515>, 2001.

879 Phillips, J.D., Lutz, J.D.: Profile convexities in bedrock and alluvial streams, *Geomorphology* 102, 554–566, doi:  
880 <https://doi.org/10.1016/j.geomorph.2008.05.042>, 2008.

881 Pilorget, C. & Forget: Formation of gullies on Mars by debris flows triggered by CO<sub>2</sub> sublimation, *Nature Geoscience*, 9, 65–  
882 69, doi: <https://doi.org/10.1038/ngeo2619>, 2016.

883 [Plaut, Jeffrey J., Ali Safaeinili, John W. Holt, Roger J. Phillips, James W. Head III, Roberto Seu, Nathaniel E. Putzig, and](#)  
884 [Alessandro Frigeri: Radar evidence for ice in lobate debris aprons in the mid-northern latitudes of Mars, \*Geophysical research\*](#)  
885 [letters 36, no. 2, doi: <https://doi.org/10.1029/2008GL036379>.](#)

886 Reiss, D. et al.: Absolute dune ages and implications for the time of formation of gullies in Nirgal Vallis, Mars. *J. Geophys.*  
887 *Res.-Planets* 109, doi: <http://dx.doi.org/10.1029/2004JE002251>, 2004.

888 Reiss, D., Hauber, E. et al.: Terrestrial gullies and debris-flow tracks on Svalbard as planetary analogs for Mars, In: Garry,  
889 W.B. & Bleacher, J.E. (eds) *Analogues for Planetary Exploration*, Geol. Soc. Am. Spec. Papers 483, 165–175, doi:  
890 [https://doi.org/10.1130/2011.2483\(11\)](https://doi.org/10.1130/2011.2483(11)), 2011.

891 Rodine, J.D., Johnson, A.M.: The ability of debris, heavily freighted with coarse clastic materials, to flow on gentle slopes,  
892 *Sedimentology* 23, 213–234, doi: <https://doi.org/10.1111/j.1365-3091.1976.tb00047.x>, 1976.

893 Ryder, J.: Some aspects of the morphometry of paraglacial alluvial fans in South-central British Columbia, *Canadian Journal*  
894 *of Earth Sciences* 8: 1252–1264, doi: <https://doi.org/10.1139/e71-11>, 1971.

895 Schon, S.C., Head, J.W., Fassett, C.I.: Unique chronostratigraphic marker in depositional fan stratigraphy on Mars: Evidence  
896 for ca. 1.25 Ma gully activity and surficial meltwater origin, *Geology* 37, 207–210, doi: <http://dx.doi.org/10.1130/g25398a.1>,  
897 2009.

898 Siewert, M. B., Krautblatter, M., Christiansen, H. H., & Eckerstorfer, M.: Arctic rockwall retreat rates estimated using  
899 laboratory-calibrated ERT measurements of talus cones in Longyeardalen, Svalbard, *Earth Surface Processes and Landforms*,  
900 37(14), 1542–1555, doi: <https://doi.org/10.1002/esp.3297>, 2012.

901 Sinha, R. K., Ray, D., De Haas, T., & Conway, S. J.: Global documentation of overlapping lobate deposits in Martian gullies.  
902 *Icarus*, 352, 113979, doi: <https://doi.org/10.1016/j.icarus.2020.113979>, 2020.

903 Sinha, R. K., Vijayan, S., Shukla, A. D., Das, P., & Bhattacharya, F.: Gullies and debris-flows in Ladakh Himalaya, India: a  
904 potential Martian analogue, *Geol. Soc. Lond. Spec. Publ.* 467, 315–342, doi: <https://doi.org/10.1144/SP46>, 2019.

905 Sinha, R.K., Vijayan, S.: Geomorphic investigation of craters in Alba Mons, Mars: implications for Late Amazonian glacial  
906 activity in the region, *Planet. Space Sci.* 144:32–48, doi: <https://doi.org/10.1016/j.pss.2017.05.014>, 2017.

907 Souness, C., & Hubbard, B.: Mid-latitude glaciation on Mars, *Progress in Physical Geography*, 36(2), 238–261, doi:  
908 <https://doi.org/10.1177/030913331243>, 2012.

909 Souness, C., Hubbard, B., Milliken, R. E., & Quincey, D.: An inventory and population-scale analysis of martian glacier-like  
910 forms, *Icarus*, 217(1), 243–255, doi: <https://doi.org/10.1016/j.icarus.2011.10.020>, 2012.

911 Stock, J.D., Dietrich, W.E.: Erosion of steepland valleys by debris flow, *Geol. Soc. Am. Bull.* 118 (9/10), 1125–1148.  
912 doi:10.1130/B25902.1, 2006.

913 Stolle, A., Langer, M., Blöthe, J. H., & Korup, O.: On predicting debris flows in arid mountain belts, *Global and Planetary*  
914 *Change*, 126, 1–13, doi: <https://doi.org/10.1016/j.gloplacha.2014.12.005>, 2015.

915 Welsh, A., Davies, T.: Identification of alluvial fans susceptible to debris-flow hazards. *Landslides* 8 (2), 183–194, doi:  
916 <https://doi.org/10.1007/s10346-010-0238-4>, 2011.

- 917 Wilford, D. J., Sakals, M. E., Innes, J. L., Sidle, R. C., & Bergerud, W. A.: Recognition of debris flow, debris flood and flood  
918 hazard through watershed morphometrics, *Landslides*, 1(1), 61-66, doi: <https://doi.org/10.1007/s10346-003-0002-0>, 2004.
- 919 Yue, Z., Hu, W., Liu, B., Liu, Y., Sun, X., Zhao, Q. and Di, K.: Quantitative analysis of the morphology of martian gullies and  
920 insights into their formation, *Icarus*, 243, pp.208-221, doi: <https://doi.org/10.1016/j.icarus.2014.08.028>, 2014.

921